Rational Design of Frontline Institutional Phage Cocktail for the Treatment of Nosocomial *Enterobacter cloacae* Complex Infections

Dinesh Subedi[1,2]*, Fernando Gordillo Altamirano[2,3], Rylee Deehan[1,4], Avindya Perera[1], Ruzeen Patwa[1], Xenia Kostoulias[2,3,5], Denis Korneev[6], Luke Blakeway[3], Nenad Macesic[2,3], Anton Y Peleg[2,3,5#], Jeremy J Barr[1,2#]*

Affiliation
1. School of Biological Sciences, Monash University, Clayton, VIC, Australia.
2. Centre to Impact AMR, Monash University, Clayton, VIC, Australia.
3. Department of Infectious Diseases, The Alfred Hospital and School of Translational Medicine, Monash University, Melbourne, Victoria, 3004, Australia.
4. Australian Centre for Ecogenomics, School of Chemistry and Molecular Biosciences, University of Queensland, Saint Lucia, QLD, Australia
5. Infection Program, Monash Biomedicine Discovery Institute, Department of Microbiology, Monash University, Clayton, Victoria, 3800, Australia.
6. Department of Biochemistry and Molecular Biology, Monash University, Clayton, VIC, Australia.

* Corresponding authors dinesh.subedi@monash.edu; jeremy.barr@monash.edu

#Authors contributed equally

SUMMARY

In brief

We developed a phage product containing five phages with frontline potential to address infections caused by multidrug-resistant *Enterobacter cloacae* complex.

Abstract

Phage therapy is a promising strategy to treat antimicrobial-resistant infections. Currently, phage therapy applications span personalised treatments that are tailored for a given patient's infection, through to the use of pre-established cocktails of virulent phages against clinically relevant pathogens. However, both approaches face challenges, with personalised phage therapy being time-consuming and requiring a phage match to a patient's infection, while phage cocktails may not be effective against a patient's specific strain. The Alfred Hospital in Melbourne, Australia has reported an ongoing outbreak of infections by the *Enterobacter cloacae* complex (ECC), a group of emerging multidrug-resistant pathogens responsible for considerable morbidity and mortality. Utilising the hospital's strain collection, built over the last decade, we established an initial three-phage product with 54% ECC coverage that effectively reduced bacterial loads (>99%) in septicaemic mice. We then iteratively improved this product by enhancing phage killing efficiency using phage training and expanded host range through targeted phage isolation against low-coverage ECC strains. This iterative optimisation led to the creation of the product *Entelli-02*, containing five well characterised virulent phages that target clinical ECC strains through distinct bacterial cell surface receptors. Importantly, *Entelli-02* exhibits broad host coverage (99%) and efficacy (92%) against The Alfred Hospital's ECC strain collection (n = 156). We produced this as a therapeutic-grade product, verified and endotoxin unit compliant, ready for use. This approach integrated academic phage research with clinical insights to produce the phage product *Entelli-02* as an institution-specific phage cocktail with frontline efficacy and on-demand availability.

Introduction

The emergence and spread of antimicrobial resistance (AMR) poses a serious threat to global health and calls for alternative strategies to combat bacterial infections[1]. Phage therapy, which involves the use of virulent bacteriophages (phages) that can infect and destroy bacteria, has garnered renewed attention as one potential solution to the AMR crisis[2]. Phage therapy offers several advantages over conventional antibiotics, such as high specificity, self-replication, low toxicity, and adaptability to changing bacterial pathogens[3]. Combinations of multiple phages, which are colloquially known as phage cocktails, are often used to broaden the antimicrobial spectrum. Phage cocktails can be produced *a priori* against a target pathogen or group of bacteria[4]. Despite these benefits, clinical trials employing phage cocktails have shown limited clinical efficacy[5-12]. Treatment failure was attributed to target strain divergence, phage stability issues, and the mismatch between phage infectivity on the bacterial isolates the cocktails were constructed upon versus the clinical strains that were eventually treated. In contrast, personalised phage therapy involves the identification and use of a phage with demonstrated activity against a patient's bacterial infection[13,14]. This approach is often followed by adapting or training the phages to improve their effectiveness, small-scale production, and bespoke treatment. While personalised phage therapy approaches have shown promising results with >70% treatment efficacy[15], their application presents the additional complexity of requiring rapid phage characterisation, safety and efficacy testing, and administration of the product, all within a practical timeline. A combination of both approaches, with the initial use of a predefined broad-spectrum phage cocktail, while transitioning to personalised approaches as needed, is an appealing strategy for rapid treatment of antibiotic-resistant bacterial infections.

To bridge the divide between broad-spectrum phage cocktails and personalised therapy, we designed a phage product that was targeted towards a high-risk, multi-clonal outbreak of a nosocomial pathogen at a local hospital. We targeted *Enterobacter cloacae* complex (ECC), which is an emerging group of nosocomial pathogens that pose a significant threat to human health due to their acquisition of virulence and AMR determinants. Classified among the ESKAPE pathogens, this complex encompasses clinically relevant species such as *E. cloacae, E. asburiae, E. hormaechei, E. kobei*, and *E. ludwigii,* which can cause diverse infections, such as pneumonia, urinary tract infections, intraabdominal infection, and bacteraemia[16,17]. Notably, these pathogens have considerable epidemic potential, having contributed to a global surge in carbapenem-resistant and extended-spectrum beta-lactamase-producing phenotypes[18], and were responsible for numerous clonal hospital outbreaks with limited treatment options[19-21].

83 As a result, ECC is increasingly associated with severe AMR infections in health care settings
84 and was associated with >200,000 deaths globally in 2019 alone[22-27].

85 The Alfred Hospital, a tertiary referral centre in Melbourne, Australia, has reported an ongoing
86 outbreak of carbapenemase-producing *Enterobacterales* infections over the last decade[23,28,29].
87 A retrospective analysis of bloodstream infections at this centre noted ECC contributed ~20
88 cases per year, with a recent surge in ECC infections from 2018-2021[29]. Given this clinical
89 burden, there is an urgent need to develop alternative treatments against this endemic,
90 nosocomial, AMR pathogen. To address this, we developed a tailored phage product that is
91 suitable for frontline use against this ECC outbreak at The Alfred Hospital. We developed a
92 standardised approach that combines academic phage research with clinical insights that was
93 backed by an extensive collection of 206 clinical ECC strains collected over the past decade.
94 This enabled the creation of *Entelli-02*, an institution-specific phage cocktail that not only
95 demonstrates frontline efficacy but ensures rapid availability of an effective antimicrobial. Our
96 approach bridges personalised phage therapy with a broad-spectrum phage product that is
97 tailored toward a given hospital's (*i.e.,* institution) pathogen profile and addresses the urgent
98 need for effective treatment options against AMR pathogens in healthcare settings.

Results

Isolation and characterisation of phages against *Enterobacter* isolates from The Alfred Hospital

The Alfred Hospital in Melbourne, Australia, has reported an ongoing outbreak of nosocomial infections with limited treatment options and high mortality rates[29]. Of particular concern is the *Enterobacter cloacae* complex (ECC), which is an emerging AMR threat with considerable epidemic potential[22]. Here, we explored the potential for phages as a frontline antimicrobial solution for The Alfred's ECC outbreak. Beginning with 206 clinical ECC isolates collected over a 10-year period, we selected a subset of 36 ECC isolates, that represent the sequence type (ST) diversity of the full strain collection (Supplementary data 1). We then constructed an initial phage library against these isolates. After isolating and purifying 21 novel phages, we screened their plaque-forming capacity against our strain subset to obtain a host range map (Fig 1A). Of the 36 isolates, 34 were susceptible to at least one phage. However, considering the time and cost associated with characterising and producing each therapeutic phage, we aimed to build a phage combination that offers the broadest host range with the fewest possible phages combinations. Based on the complementary broad-spectrum host range, we selected øEnA02, øEnC07 and øEnC15 to produce the initial ECC phage combination (cocktail-V1), which provided 61% coverage against the 36 sub-selected ECC hosts (Fig 1A). All phages in the cocktail were sequenced and their genomes were analysed to ensure they did not carry genes known to allow lysogeny or virulence, including integrases, recombinase, mobile genetic elements, or genes encoding antibiotic resistance or toxicity. Based on genome similarity, we classified the phages at the genus level (Supplementary Fig 1 and 2, Fig 1B). Electron microscopy imaging (Fig 1C-E) revealed icosahedral capsids and sheathed contractile tails with lateral tail fibres, consistent with the Tevenvirinae subfamily within the *Straboviridae* family[30]. Importantly, therapeutically relevant bacteriophages must effectively supress target strains and be capable of efficient replication. We evaluated the replicative characteristics of the three phages on their host of isolation using the one-step growth curve, revealing that øEnA02 had a burst size of 86 per infected cells with a latency of 20 minutes (Fig 1F), øEnC07 had a burst size of 40 with a latency of 20 minutes (Fig 1G), and øEnC15 had a burst size of 349 with a latency of 15 minutes (Fig 1H). Next, we verified the killing efficacy of the three phage cocktail as assessed by efficiency of plating (EOP) to evaluate how well the cocktail phages could infect other permissive hosts[31]. The results demonstrated EOPs between 0.1 and >1 for all interactions between cocktail phage and permissive hosts except for two instances: øEnA02 against CPO239 and øEnC15 against CPO053 (Fig 1I). Notably, in each case of

permissive host interaction, at least one phage in the cocktail exhibited an EOP of 20% or higher.

As we were aiming to produce a frontline antimicrobial preparation, phage stability under variable storage conditions is paramount[32,33]. We examined the stability of each phage within the cocktail under storage conditions at 4 °C, room temperature (~22 °C), and 37 °C for 30 months and performed phage titrations at different intervals. Within the initial six months, no noticeable drop in titre occurred in lysates stored at 4 °C and room temperature, with 4 °C proving the most stable condition and maintaining phage stability for up to 30 months. Phages stored at 37 °C were the least stable, losing therapeutic titre within two months (Fig 1J). Collectively, these data suggest that these three phages have broad host range and high antimicrobial efficacy against ECC isolates, and demonstrate excellent stability, making them promising candidates for further development and evaluation.

Figure 1. Formulation and characterisation of a three-phage combination (A-J)

(A) Host range map of isolated phages (columns, $n = 21$) tested against a subset of 36 *Enterobacter cloacae* complex (ECC) isolates. Each row represents an ECC isolate, classified based on Sequence Type (ST), and is colour-coded accordingly. Singletons are STs that only occurred once.

(B) Representations of phage genome size and classification of the three phages (øEnA02, øEnC07 and øEnC15) of the cocktail.

(C-E) TEM images of the three phages (øEnA02, øEnC07 and øEnC15), with a 100 nm scale bar.

(F-H) One-step growth curve of the three phages (øEnA02, øEnC07 and øEnC15) in the cocktail. Each point represents the average of three independent experiments, and the error bars indicate the standard error of the mean. The latency time (in minutes) and burst size (in PFU/infection) were calculated for each phage.

(I) Relative efficiency of plating (EOP) values for three phages, represented by different coloured dots, across ECC isolates. The dotted line represents the EOPs on the host of isolation, which is set as 1. LOD = limit of detection.

(J) Stability of the three phages (øEnA02, øEnC07 and øEnC15) in 4 °C, room temperature and 37 °C, storage conditions. LOD = limit of detection, M = months.

Identification of Phage Receptors

Bacteria can quickly evolve resistance against phage predation; this typically manifests via loss-of-function mutations in the surface-associated structures that phages adsorb to. The simultaneous use of diverse phages targeting different bacterial surface structures can minimise or delay the evolution of phage-resistance[34,35]. To identify the receptors involved in phage-host interactions, we generated phage-resistant mutants which were sequenced to identify loss-of-function mutations[36]. We identified putative phage receptors by mapping the raw reads of phage-resistant mutants to the wild-type genome. To validate these phage-receptors, we complemented the candidate wild-type (WT) gene back to its respective phage-resistant mutant and performed an adsorption assay to determine whether phage infectivity was restored. We found that each of the three phages targeted a different component of the lipopolysaccharide (LPS) structure (Fig 2A).

174 In the phage resistant mutant øEnA02, we identified two loss of function mutations, the first
175 (Fig 2B) in *wcaJ,* which is an O-antigen-associated gene[37], and the second in an outer
176 membrane protein (*ompW*) (Fig 2C), with both mutations resulting in the gain of an early stop
177 codon. O-antigen is a serogroup-specific sugar-based component of the outer LPS layer of
178 Gram-negative bacteria and is a well-characterised phage receptor[38-40]. OmpW has been shown
179 to be a phage receptor for *Vibrio cholerae* phage[41-43], has important roles in virulence, and acts
180 as a colicin receptor in *E. coli*, suggesting a potential fitness trade-off associated with phage-
181 resistance[42,43]. Following complementation, we quantified øEnA02 adsorption to the WT-host,
182 each of the two phage-resistant mutants, and each mutant complemented with the respective
183 WT gene. The WT-host adsorbed approximately 1 log of phage within 10 minutes, while both
184 phage-resistant mutants showed minimal adsorption (Fig 2B and 2C). Comparatively, the
185 complemented strains restored phage adsorption albeit only partially for the OmpW mutant
186 (Fig 2C), suggesting that øEnA02 may use OmpW as a secondary receptor.
187 The øEnC07-resistant mutant had a loss-of-function mutation in a glycosyltransferase gene,
188 which is a part of *rfa* operon and associated with LPS core synthesis[44,45]. Complementing the
189 mutant with the WT gene restored phage infectivity and increased phage adsorption by 0.2 log
190 (Fig 2D). Finally, øEnC15-resistant mutant had a stop codon in the UTP-glucose-1-phosphate
191 uridyltransferase gene (*galU*), which encodes an enzyme for UDP-glucose synthesis, which is
192 a precursor for O-antigen synthesis[46]. Complementing *galU* into the phage-resistant mutant
193 restored phage adsorption, indicated by a 0.6 log increase (Fig 2E). The identification of phage
194 receptors provides mechanistic insights into phage infectivity and the emergence of resistance.
195 While all our phages broadly targeted the LPS, this was mediated through different LPS
196 subunits, which likely reduces the emergence of phage resistance when used in combination
197 (Supplementary Fig 3).

198 Figure 2. Receptors of three phages of cocktail-V1 (A-E)
199 (A) Schematic representation of the *Enterobacter* lipopolysaccharide (LPS) and membrane structure,
200 with validated phage receptors indicated by arrows. Colours are for illustrative purposes only and
201 the faded section represents the potential loss of LPS structure in phage resistant mutants. Figure
202 drawn based on[47].
203 (B-E) Single nucleotide polymorphisms (SNPs) identified in the genomes of phage-resistant mutants
204 and their predicted effects. ø-R-mutant indicates phage-resistant mutant, numbers represent
205 nucleotide positions. Graphs on the right of each panel show phage adsorption assays testing the
206 ability of phages to adsorb to their corresponding wild-type (WT), phage-resistant mutant, and
207 complemented hosts over 10 minutes. Each point on the graph represents the average of three
208 independent experiments, and the error bars indicate the standard error of the mean.

In-vivo effectiveness of the preliminary phage combination (cocktail-V1)

After establishing the host range, infectivity, genomes, stability, and receptors for our preliminary three-phage combination (cocktail-V1), we evaluated its efficacy in reducing ECC burden *in vivo* using a murine model. For this model, we selected ECC isolate APO57, which was susceptible to all three phages at an EOP ~1. We optimised the ECC inoculum dose to induce severe septicaemia in 8-weeks-old BALB/c mice, reaching an ethical endpoint within 12 hours (Supplementary Fig 4). Mice were intraperitoneally (IP) injected with 200 µL of an optimised dose of 5×10^6 CFU/mL of strain APO57. One hour-post-infection (hpi), mice were treated with a single dose of cocktail-V1, which contained 10^8 PFU/mL of each three phages at in 200 µL, while control mice received an equivalent volume of sterile PBS. The experiment concluded at 12 hpi and vital organs were collected to assess the bacterial and phage load (Fig 3A). The phage-cocktail treatment resulted in >3 log reduction (>99.9%) in the bacterial burden in the infected mouse's blood, kidney, liver, and spleen compared to the PBS control group ($p < 0.05$) (Fig 3B). Notably, bacterial load in the blood was cleared below our detection limit (2 log) in four out of six mice. Phage load assessment revealed propagation of all three phages *in vivo*, indicating successful replication and dissemination throughout the mice (Fig 3C). We further observed that the liver and spleen exhibited higher phage concentrations compared to the blood and kidney ($p < 0.05$). However, there was no significant difference in phage concentrations when comparing the blood to the kidney or the liver to the spleen. Due to its capacity to reduce bacterial burden and ability to replicate effectively in mouse organs, we advanced the three-phage combination to the next stage of clinical evaluation.

Figure 3. Efficacy of the phage cocktail-V1 against mouse infections and its host coverage across a range of clinical isolates (A-D).

(A) Experimental scheme for the animal experiment. Grey numbers represent number of mice, black numbers represent hours post-infection.

(B) The reduction of bacterial load in vital tissues of treated mice compared to the control group. Each data point represents the results from an individual mouse ($n = 6$), and the median and interquartile range are shown. Total represents data from all samples ($n = 24$) combined. Statistical analysis was performed using the Mann-Whitney U test to assess the differences between medians of bacterial count.

(C) The propagation of three different phages in various tissues of treated mice. The data ($n = 6$) are shown in box plots, with medians, interquartile range, and outliers (points beyond whisker) shown. Statistical analysis was performed using the Mann-Whitney U test to assess the differences between medians of phage titre in each tissue.

(D) Host range map of cocktail V1 (øEnA02, øEnC07, and øEnC15) and its individual components tested against 120 *Enterobacter cloacae* complex (ECC) isolates from The Alfred Hospital. Each column represents an ECC isolate, classified based on their Sequence Type (ST), and is color-coded accordingly. Red boxes indicate complete phage lysis of the respective ECC isolate, yellow boxes represent partial phage lysis (hazy zone), and light blue boxes indicate no observed lysis.

Efficacy of cocktail-V1 against the wider collection of clinical ECC isolates

At this stage, we wanted to determine the effectiveness of our phage cocktail-V1 against the broader clinical collection of ECC isolates from the Alfred Hospital. We screened the lytic activity of our phage cocktail and its individual components via a spot assay against 120 clinical ECC isolates (Fig 3D). At the time, this represented the entire ECC collection at The Alfred, encompassing a diverse range of sequence types (STs) that contributed to the nosocomial outbreak. Two researchers who were blinded to the experiment visually scored the zones on the bacterial lawn as complete lysis (phages clearing the bacteria), hazy (bacteria partially cleared) or no lysis (no effect of phages) (Supplementary Fig 5). The three-phage cocktail completely lysed 54.2% of the 120 ECC isolates, which was a decrease of ~7% in lysis when compared against the initial 36 isolate collection cocktail-V1 was built upon (Fig 1A). Hazy spots (~45%) were not confirmed for productive infection via the soft overlay (top) agar assay, but likely represented a combination of low EOP, phage resistance and bactericidal activity resulting from "killing from without"[48]. We also observed association between phage susceptibility and ST of the ECC isolates, with ST-114, 190 and 1015 being the least susceptible to the cocktail. The modest host range coverage of 54.2%, along with limited activity against specific STs, underscored the need for a more tailored approach to phage isolation and the refinement and expansion of phage infectivity to ensure comprehensive coverage across broader STs encompassing the ECC nosocomial outbreak.

Phage training to improve adaptability and infectivity.

A fundamental difference between phages and antibiotics is phages can evolve and adapt to changes in their hosts. This can be harnessed to train phages and achieve improved fitness and therapeutic efficacy[49-51]. Using an experimental evolution approach, we set out to improve the lytic capacity of the three phages from cocktail-V1. Our first goal was to determine the optimum phage training duration that would result in improved lytic capacity. We selected ECC strain AH17D011 and øEnC07, a phage-host pair with a moderate EOP of 0.79. Following 24 hours of propagation, we purified the population of trained phages, which were then used to infect a naive host population, with the entire process being repeated for 10 days. After five days, we performed a growth kinetics assay to determine the lytic efficacy of the phages and calculated phage scores as an indicator of phage fitness[52,53]. We observed that the phage score increased sharply starting on day five of training and plateaued afterwards (Supplementary Fig 6). Based on these observations, we determined that the optimum phage training period was between five to seven days, with seven days being selected for further

282 experiments. Importantly, following the seven-day phage training, evolved phages were twice
283 single-plaque purified to ensure that a single phage genotype was taken for downstream
284 characterisation, including lytic activity via EOPs, growth curve, and genomic changes (Fig
285 4A).
286 We then examined whether phage training could enhance lytic activity against hosts that had
287 lower EOPs and were less responsive to a specific phage. As such, we trained the remaining
288 two phages from our cocktail: øEnA02 with host AH19K020, (EOP 0.2), and øEnC15 with the
289 apparently non-permissive host CPO390 (EOP below the limit of detection). Following phage
290 training, EOPs improved by 4,000-fold for øEnA02 (p <0.001) and 8.7-fold of øEnC07 (p =
291 0.033) against their training hosts. Intriguingly, øEnC15, initially incapable of productive
292 infection on its training host, was found to infect it and propagate therein at an EOP of 0.4 after
293 training (Fig 4 B-D). To evaluate the broader fitness of trained phages and any potential trade-
294 offs, we compared their lytic activity to that of their ancestral counterparts across our 36 ECC
295 isolate subset. The evolved phages showed an increased average phage score for øEnC07 (p =
296 0.078) and øEnC15 (p = 0.048), while øEnA02 showed minimal change (p = 0.84) (Fig 4E,
297 Supplementary Fig 7).
298 To determine whether the observed improvements in the killing efficiency of the evolved
299 phages were accompanied by changes in their life cycles, we conducted one-step kill curves on
300 their training hosts. Compared to its ancestor, the evolved øEnA02 had a faster replicative cycle
301 as demonstrated by a shorter latency period (20 min vs 26 min) and released more progeny
302 virions (burst size; 21 vs 15) (Fig 4F). Evolved øEnC07 showed an enhanced adsorption rate,
303 as indicated by the steeper decline of free phage percentage in the first 15 minutes of infection,
304 with a comparable latency (22 min vs 20 min) and larger burst size (19 vs 11) (Fig 4G). As for
305 the øEnC15, we lacked an ancestral phage that could infect the host for the comparison, so we
306 evaluated the life cycle parameters of the evolved generation, revealing a latent period of about
307 18 min and a burst size of 10 (Fig 4H).
308 To explore the molecular mechanisms underlying the improved phage efficacy, we conducted
309 genome sequencing and comparative analysis between the evolved phages and their ancestors
310 (Supplementary Fig 8). We identified several SNPs in the evolved phages, with the majority
311 located in the tail region of the genome, including the tail fibre and receptor-recognising
312 proteins. These proteins are critical for the initial adsorption of phages to host bacteria.
313 Interestingly, we found that some of the SNPs were unique to certain phage-host pairs,
314 indicating the specificity of the evolutionary process. Based on our observation, we
315 hypothesised that the improved phage efficacy resulted from selection and accumulation of

316 beneficial mutations during the training process, which enabled the phages to better recognise
317 and bind to their hosts. Collectively, these results demonstrate that our phage training approach
318 successfully improved phage infectivity against inefficient or even non-permissive hosts, via
319 mutations in phage tail structures, impacting divergent variables of the phage lifecycle and
320 enhancing killing efficiency.

321 Figure 4. Phage training and its effect on phage adaptation (A-H).
322 (A) Experimental protocol for phage training. Ancestral phage was propagated with training hosts for 24
323 hours. Subsequently, the purified phage population was repropagated on a naive population of the same
324 training host, with this cycle repeated for 10 days. After five days, daily measurements of phage growth
325 curves were conducted using the evolved population to find the optimum training duration. The final
326 evolved phages (i.e., day 7) were isolated via double single-plaque purification to obtain an individual
327 genotype of phage mutants. Then, the growth characteristics of these single genotype evolved phages
328 were assessed.
329 (B-D) The relative efficiency of plating (EOP) of evolved phages (øEnA02, øE2nC07, and øEnC15)
330 compared to their ancestral counterparts. The labels on top of the boxes represent the training ECC host.
331 Each point (n = 6) represents data from independent biological replicates. p values were calculated by a
332 two-tailed t-test with Welch's correction. Box bounds indicate 25th and 75th percentile.
333 (E) Phage score of ancestor phages compared with their respective evolved phages, tested against a subset
334 of 36 *Enterobacter cloacae* complex (ECC) isolates. Each dot represents a phage score (n = 36). p values
335 were calculated by a two-tailed t-test with Welch's correction.
336 (F-H) One-step growth curve of evolved phages (øEnA02, øE2nC07, and øEnC15) compared to their
337 ancestral counterparts, on their respective training hosts. Each point represents data from independent
338 biological replicates (n = 3), and the error bars indicate the standard error of the mean.
339
340

341 **Targeted phage isolation against problematic sequence types (STs).**

342 Thus far, we focused on characterising three phages of our cocktail-V1 and demonstrated their
343 *in vitro* and *in vivo* efficacy, followed by phage training to improve their lytic capacity on low-
344 EOP hosts. However, this three-phage combination had limited effectiveness against specific
345 STs from the ECC collection (Fig 3D). To address this, we selected ECC strains from STs that
346 lacked sufficient phage coverage as hosts for targeted phage isolation. Five novel phages were
347 isolated, and their activity tested via spot assay (Supplementary Fig 9). Based on the host range
348 map and complementary spectrum of activity provided by cocktail-V1, we selected two
349 candidate phages (øNando and øTaquito) for further characterisation (Fig 5A). Genomic and
350 taxonomic classification revealed both phages belonged to the Genus *Pseudotevenvirus* under
351 the Straboviridae family (Fig 5B). TEM confirmed the presence of an icosahedral head (70-75
352 nm diameter) and a long contractile tail (210 nm), consistent with the characteristics of the
353 Straboviridae family (Fig 5C and 5D). The genomes of both phages lack transposase or
354 integrase genes, antimicrobial resistance markers, and virulence genes, indicating that they are
355 not temperate and are suitable candidates for therapeutic use.
356 Identification of receptors revealed that both phages targeted different bacterial cell surface
357 structures to mediate infection (Fig 5E). For the øNando-resistant host (mutated from strain
358 CPO448), we found a loss of function mutation within *wzzB*, which encodes a protein involved

359 in the biosynthesis of O-antigen and helps determine the chain length[54]. Additionally, for
360 øTaquito, we discovered a loss-of-function mutation in a resistant variant of host CPO165
361 within the *rfaQ* gene. RfaQ is involved in LPS biosynthesis as it transfers the first two heptose
362 residues in the inner core of LPS, and its loss leads to a severely truncated LPS alongside
363 pleiotropic effects on bacterial cells[44]. We next evaluated one-step growth curves for both
364 phages, with øNando demonstrating a burst size of 88 and a latency of 15 minutes (Fig 5F) and
365 øTaquito a burst size of 13 and a latency of 20 minutes (Fig 5G). Regarding stability, both
366 phages when stored at 4 ºC maintained stability for up to 18 months (Fig 5H), whilst room
367 temperature storage supported phage stability for at least six months. These findings, combined
368 with our initial phage results, warranted the inclusion of these two additional phages to our
369 cocktail aiming towards an expanded host range with coverage against problematic STs that
370 cocktail V1 did not target.

371 Figure 5. Targeted phage isolation and expansion of host range (A-H).
372 (A) Host range map of isolated phages and cocktail-V1 tested against the initial subset of 36
373 *Enterobacter cloacae* complex (ECC) isolates. Each row represents a phage. Sequence Types (ST) are
374 colour coded. Singletons are STs that occurred once. Red boxes show phage lysis and light blue boxes
375 show no lysis.
376 (B) Representations of phage genome size and classification of the phages (øNando and øTaquito).
377 (C and D) TEM images of the two phages. Scale bar = 100 nm.
378 (E) Schematic representation of the *Enterobacter* lipopolysaccharide (LPS) and membrane structure,
379 with putative phage receptors indicated by arrows. Colours are for illustrative purposes only and the
380 faded section represents the potential loss of LPS structure in phage resistant mutants. Figure drawn
381 based on[47].
382 (F and G) One-step growth curves of øNando and øTaquito. Each point represents the average of three
383 independent experiments, and the error bars indicate the standard error of the mean.
384 (H) Stability tracking of øNando and øTaquito over 18 months, with storage at 4 ºC (solid line) and
385 room temperature (dotted line).
386

387 Improved five-phage cocktail achieved broad coverage against clinical 388 ECC isolates.

389 Our first-generation, three-phage cocktail (cocktail-V1) achieved a modest ~54.2% host range
390 coverage against the ECC isolates endemic to The Alfred Hospital. To improve its coverage
391 and efficacy, we trained the original three phages to enhance their lytic activity against selected
392 low-EOP hosts, followed by a targeted isolation of two novel phages against problematic STs.
393 Our focus then shifted to identifying the optimal combination of these phages for the
394 development of an improved cocktail. To this end, we prepared eight combinations of phages
395 comprising three-, four-, or five-phage combinations from the above mentioned eight candidate
396 phages (three ancestral phages, three evolved phages, and two targeted-isolation phages). We
397 tested these cocktails and PBS control (nine samples labelled A-I) using a spot assay against
398 an expanded collection of 156 clinical ECC strains, which included our previous panel (*n* =

120) (Fig 4D) plus 36 additional strains that caused infections in the hospital during the timeline of this study.

Both of our five-phage combinations: combination G utilising evolved phages (ev_øEnA02, ev_øEnC07, ev_øEnC15, plus phages øNando and øTaquito) and combination I with ancestral phages (øEnA02, øEnC07, øEnC15, øNando and øTaquito) produced complete lysis on spot assays against ~65% and 75% of the collection, respectively. These ranges included isolates from ST 114 and other previously untargeted STs, therefore surpassing the performance of other combinations (Fig 6A; Supplementary Fig 10). This marked a substantial improvement over cocktail-V1's 43.9% spot lysis on the expanded collection of strains. Next, to resolve whether hazy spots were indicative of productive infection, we used growth kinetics assays and calculated phage scores. We selected 67 hosts for analysis, including all hosts where either both or any of combinations G and I created hazy spots, and a few hosts with complete lysis as controls. To distinguish productive infections, optimum cut-off value of 0.28 in phage score was determined using the maximum likelihood estimation[55]. The majority of the hosts with hazy zones on spot assays yielded productive infections except for 12 instances in cocktail G and 9 in cocktail I. All instances of complete lysis spots were confirmed to be productive, except for one in combination G. Additionally, no difference in the phage score was observed between G and I (Fig 6B). Combining these results with the spot assay data, we deduced that both G and I achieved a lysis rate of at least 92% (144 out of 156 isolates) (Fig 6C). However, given our previous demonstration of enhanced fitness of the evolved phages compared to their ancestral counterparts (Fig 4E), combination G was selected for manufacturing of stable, therapeutic-grade phage product.

Production of a therapeutic-grade phage cocktail *Entelli-02*

We manufactured a therapeutic-grade phage product that we named "*Entelli-02*" from the five-phage combination (G) at our in-house facility, the Monash Phage Foundry (Fig 6D). In a first stage, we produced each phage individually. Here, phages were amplified through overnight propagation with their respective ECC hosts of isolation. The resulting phage lysates were processed using a two-stage sequential depth filtration (0.5-15 µm and 0.2-3.5 µm retention ratings) to reduce bacterial biomass followed by sterilising grade (0.2 µm) filtration into sealed glass containers. Bacteria-free lysates (approximately 1 L each) were then transferred to a clean-room facility for further processing. Phage lysates were diluted ~10-fold in 1X PBS followed by buffer exchange and concentration using tangential flow filtration (TFF), resulting in a recovery between 130 -160 mL of washed and concentrated lysate from each production

run. We observed a recovery efficiency ranging from 24% to 76%, with a PFU/mL count exceeding 10^{10} PFU/mL for each phage (Fig 6D) (Supplementary Table 1).

In stage two of production, we mixed and, if necessary, diluted the five concentrated lysates to achieve a uniform phage product with a titre of $>10^9$ PFU/mL per phage in a total of 75 mL. We then depleted endotoxin using both EndotrapHD and 1-Octanol treatments, resulting in nearly 10-fold reduction in endotoxin levels (Fig 6E). Finally, we diluted the cocktail ten-fold in 1X PBS to obtain our final product consisting of an average titre of $\sim 5 \times 10^8$ PFU/mL/phage in a total volume of 500 mL. The cocktail was twice filter-sterilised using sterilising-grade filters (0.2 μm), followed by quality control validation for phage titre and endotoxin levels (see detailed methods). The cocktail was then packaged into syringe-accessible vials, each containing 35 mL of *Entelli-02*, which is suitable for a two-week treatment course with an effective dose of 1 mL administered twice daily (b.i.d.). The final packed product underwent external validation for sterility and endotoxin, according to the USP71 and USP85 guidelines, respectively, with >10% of the production batch sent for validation. The final product contained no visible growth of microorganisms and had an endotoxin concentration of 1,575 EU/mL, which according to FDA guidelines (5 EU × kg × h) would be safe for intravenous administration b.i.d. to a patient >30 kg[56]. Electron microscopy images confirmed the visual integrity and cleanliness on *Entelli-02* (Fig 6F). Furthermore, considering these phages were amplified on clinical isolates, we also performed whole genome sequencing of the final product, followed by read mapping to the individual phage genomes, the host bacterial genomes, and predicted prophage regions (see Methods). Sequence analysis showed that >99.2% of reads mapped to the phage genomes, 0.27% to the bacterial genome, and about 0.08% to predicted prophage regions (Supplementary Table 2). To further, examine the prophage presence, we determined the normalised coverage per million reads (relative abundance) of five phages and predicted prophages. Considering the average titre of $\sim 5 \times 10^8$ PFU/mL/phage in our product and based on the relative abundance of 0.7 (0.01%) of prophage genomes (Fig 6), we inferred that the level of prophage in *Entelli-02* is $<5 \times 10^4$ PFU/mL. Finally, an important aspect of the chemistry, manufacturing, and control process is maintaining the stability of the individual components over time. We measured titre of the individual phages using selective platting within our final *Entelli-02* product and found no indication of stability issues over 6 months of storage at 4 ˚C (Fig 6G). In summary, these tests confirmed the suitability of *Entelli-02* for compassionate-use and rapid frontline deployment for the treatment of ECC infections originating from The Alfred Hospital.

465 Figure 6. Phage combination screening and manufacturing and quality control of phage product (A-I)
466 (A) Host range coverage of phage combinations (G and I) tested against 156 *Enterobacter cloacae*
467 complex (ECC) isolates based on spot assay data.
468 (B) Comparison of phage score of combinations G and I against *Enterobacter cloacae* complex (ECC)
469 isolates. Each dot represents a phage score (n = 67). p values were calculated by a two-tailed t-test
470 with Welch's correction. Dotted line (<0.28) indicates the threshold for characterising a phage
471 activity as productive.
472 (C) Host range coverage (n = 156) of phage combinations (G and I), based on combined phage score
473 and spot assay data.
474 (D) Schematic representation of the therapeutic-grade phage production protocol.
475 (E) Phage titre at each production steps stage. Each data point represents results from a replicate ($n \geq$
476 3), whiskers indicate maximum and minimum values, box bounds indicate 25th and 75th
477 percentile, with centre line indicating the median.
478 (F) Endotoxin activity as Endotoxin Unit (EU) per mL of pure lysate [stage 2(iii)] and the final
479 product [stage 2(vi)].
480 (G) TEM images of phage product (*Entelli-02*) showing intact virions and no contaminants.
481 (H) Phage titre stability of the packed product on storage at 4 ˚C over six months.
482 (I) Normalized relative coverage (relative abundance) of sequencing reads from the whole genome of
483 *Entelli-02* to component phages and predicted prophages.
484

485 **Discussion**

486 Currently, the lack of standardised and readily available phage products for use against
487 nosocomial multidrug-resistant pathogens is a major impediment to administering effective
488 phage therapy in healthcare settings[57]. Here, we employed a unique approach that leverages
489 the utility of broad-spectrum phage cocktails with the increased efficacy and specificity found
490 in personalised phage therapy. We define this approach as an 'institutional cocktail' that has
491 been designed upon a high-quality and representative collection of nosocomial pathogens, and
492 that can be employed locally and rapidly as a frontline therapeutic with high probability of
493 antimicrobial activity. Our integrated academic-clinical approach was personalised towards the
494 endemic pathogen profile at the institutional level and aimed to improve both the treatment
495 efficacy and response time for future compassionate-use phage therapy cases. Through this,
496 we developed an institutional cocktail, which we named *Entelli-02,* to serve as a frontline
497 therapeutic against AMR *Enterobacter cloacae* complex (ECC) infections at The Alfred
498 Hospital, in Melbourne, Australia. We envision this approach being employed to treat other
499 nosocomial pathogens, expanded across additional institutions, and iterated upon to improve
500 product efficacy towards an everchanging pathogen population.

501 Phage therapy has made significant progress in recent years. Personalised phage therapy
502 approaches have reported clinical improvement in ~75% of patients, bacterial eradication in
503 ~60-80% of patients, and adverse events in ~15% of patients[8,15]. However, personalised phage
504 therapy applications are time-consuming, complex to administer, and difficult to scale, which
505 limits the number of patients that can be treated. Conversely, broad-spectrum phage cocktails
506 designed to treat entire pathogen complexes as stand-alone therapies have been produced under

507 current pharmaceutical GMP-guidelines and can be made rapidly available. Yet the
508 performance of these defined cocktails in randomised controlled trials completed to date has
509 been underwhelming[2,8-12], hinting at a disconnect between the strains used to develop these
510 products and the clinical strains in patient cohorts being treated. While the mixing of phages
511 that target multiple strains of a single species or even multiple species is a traditional and
512 widely used method, there are several factors that can compromise the efficacy of such broad-
513 spectrum cocktails[8]. For instance, building the cocktail using limited culture collections or the
514 use of clinically irrelevant hosts may result in poor coverage and inefficient killing.
515 Additionally, the laboratory-based phage-host match may not necessarily correlate with the
516 lytic activity of the phage *in vivo*, and bacteria can quickly evolve phage resistance.
517 Importantly, few broad-spectrum cocktails identify the phage-receptors their constituents use[58],
518 with the simultaneous use of phages targeting the same receptor possibly resulting in phage
519 competition for adsorption, further reducing the cocktail's efficacy. Thus, it is important to
520 implement a rational approach for the selection of phages in a cocktail, ensuring a broad host
521 range, high efficacy, and minimal risk of resistance development[58-61].
522 For the iterative development of *Entelli-02*, we began by isolating phages against a sub-
523 collection of 36 genetically diverse isolates of ECC, representative of the broader endemic
524 ECC outbreak at The Alfred Hospital. From this initial phage library, we formulated a first-
525 generation three-phage combination (cocktail-V1) based on orthogonal host range coverage
526 and lytic activity. We then comprehensively characterised each phage for therapeutic
527 relevance, which included conducting one-step growth curves, efficiency of plating (EOP),
528 stability, genome sequencing, phage receptor validation, and *in vivo* antimicrobial efficacy.
529 The observed 3 $\log_{10}$ reduction of ECC in our *in vivo* mouse model indicates high efficacy of
530 cocktail-V1. Furthermore, these phages appear to use at least two different receptors, OmpW
531 and LPS, and importantly, different subunits of the LPS molecule. This target receptor diversity
532 makes the combined use of these phages less likely to result in inter-phage competition and
533 selection for phage-resistance. This latter point was evidenced by the apparent propagation of
534 all three phages in our *in vivo* mouse model (Fig 3C). Screening this first-generation cocktail
535 against the wider clinical collection of 120 ECC isolates revealed a moderate host range
536 coverage of 54%, with low killing efficiency against a few particular STs. Based upon these
537 results, we decided to improve our phage cocktail by iterating upon our experimental design
538 through two different approaches: first, a phage training protocol to improve the lytic activity
539 of our original phages and, second, the targeted isolation of novel phages against those low-
540 coverage STs.

541 To improve the killing efficiency, we employed an experimental evolution approach, more
542 commonly known as phage training [49-51]. Phage training would help improve the adaptability
543 of phages to other hosts, while hopefully maintaining their capacity to infect original hosts [62-
544 65]. Post-training, we isolated and characterised single phage genotypes from the evolved
545 populations. We emphasise the importance of isolating and characterising well defined,
546 singular phage genotypes from phage training techniques. It's essential to only use known
547 phage genotypes in therapy to ensure it's safe and meets regulatory requirements. Selection of
548 trained phages was based on improved phage score[66], which eventually showed improvement
549 of EOPs, improved adsorption, latency, and burst size, compared to untrained ancestors.
550 Notably, even in a case of a seemingly non-permissive host, a trained phage adapted to it,
551 resulting in efficient lysis. Coevolutionary interactions between bacteria and phage usually
552 involve adaptations to the initial adsorption of the bacteriophage to its hosts, often through
553 changes in its tail structure [67]. As expected, we observed mutations within phage tail fibre genes
554 in our trained phages. Notably, we also identified mutations in other structural genes, which
555 could impact the phage lifecycle and warrant further investigation. By combining phage
556 training with careful phenotypic selection, we improved the killing efficiency of our phages.
557 To broaden the spectrum of cocktail-V1, we employed targeted phage isolation against clinical
558 ECC strains with STs not covered by the initial cocktail. This expanded our phage library and
559 allowed us to select two additional phages that targeted different regions or potentially different
560 variant of the O antigen in LPS[68]. This selection complemented the host range of cocktail-V1.
561 Similar to the cocktail-V1 components, these phages exhibited high antimicrobial efficacy *in*
562 *vitro* and lacked lysogeny and virulence-related genes. Their inclusion enhanced our cocktail's
563 ability to target elusive STs, resulting in a widened host range practically covering the entire
564 ECC collection from the Alfred, demonstrating the importance of optimising and personalising
565 phage cocktails for specific pathogens and epidemiological niches. We also emphasised the
566 importance of regularly updating the phage cocktails based on the evolving genetic background
567 of clinical isolates to ensure the best efficacy in phage therapy.
568 *Entelli-02*, our second version phage cocktail, was selected by screening different candidate
569 combinations of phages against the entire cohort of ECC isolates via spot and bacterial growth
570 kinetics assays. The best performing combination comprised our three evolved phages plus the
571 two phages isolated against targeted STs (Fig 6A). While the host range of this combination
572 was marginally narrower than the combination containing the three ancestral phages, the
573 evolved phages showed higher adaptability to hosts, as evidenced by decreased latency period,
574 increased burst size and adsorption, which resulted in higher phage scores for two out of three

evolved phages (Fig 4E). Furthermore, evolved phages, trained on selective hosts, maintained their infectivity across the broader collection of ECC isolates, indicating no fitness trade-off for the evolved phages.

In preparation for clinical administration, we manufactured a clinical-grade *Entelli-02* and ensured a final stable product. Our production pipeline maintained high recovery efficiency and implemented traceable manufacturing procedures, ensuring consistency and reliability throughout the manufacturing process. The conclusive assessment of *Entelli-02*'s wide host coverage (~92%) on clinically relevant ECC strains further substantiates its clinical potential and capacity for rapid deployment. In summary, our study represents a comprehensive and multifaceted approach to generating an 'institutional cocktail' *Entelli-02* that bridges the gap between personalised phage therapy and broad-spectrum phage cocktails. Developed in response to a local hospital's outbreak and based on a clinically curated strain collection, *Entelli-02* is designed to combat an endemic AMR pathogen in a nosocomial setting as a frontline therapeutic. Importantly, this 'institutional cocktail' offers a streamlined alternative to the extensive processes typical of personalised phage therapies, which leverages advantages from both single-patient compassionate use and broad-range phage cocktails, setting the blueprint for establishing 'institutional cocktails' against other AMR pathogens across different hospitals and institutions. Further work is needed to determine the breadth and activity of our ECC phage cocktail against both national and international ECC isolates, including conducting clinical trials to evaluate its efficacy and safety in treating AMR ECC infections at The Alfred Hospital. Finally, this approach can be iterated and adapted to the changing genetic background of ECC clinical isolates at The Alfred Hospital, allowing us to produce future improved versions of the *Entelli-02* cocktail.

598 # Methods
599
600 ***Enterobacter cloacae* complex (ECC) clinical isolates**
601 This study used clinical isolates of *Enterobacter cloacae* complex (ECC) from The Alfred
602 Hospital, Melbourne, Australia, collected between 2010 and 2021. In total, the repository at
603 The Alfred Hospital contained 206 bacterial strains. For initial phage isolation and analysis,
604 we selected a subset of 36 strains to represent the sequence type (ST) diversity of whole
605 collection set. To further the scope of our investigation, the study was expanded to include up
606 to 156 isolates to evaluate phage and cocktail activities. No patient data were collected or used
607 in these experiments and all strains were retrieved without identifiable patient data. Strain
608 details are listed as Supplementary Data 1.
609 **Bacterial strains, plasmids and growth conditions**
610 We used lysogeny broth (LB) - 10 g/L tryptone (Oxoid Ltd, Basingstoke, UK), 5 g/L yeast
611 extract (Merck Life Science Pty Ltd; Darmstadt, Germany), 10 g/L NaCl (Merck) to grow
612 bacteria, unless otherwise mentioned. Agar (Merck) at a concentration of 15 g/L was employed
613 for agar plates and 7.5 g/L for the creation of a soft agar double-layer (top agar). All bacterial
614 cultures were grown aerobically at 37 ºC overnight. We used Omnipur phosphate-buffered
615 saline (PBS) (Merck) for all experiments unless otherwise mentioned. In gene transformation
616 experiments, we used vector pBBRMCS[69] and *E. coli* DH5-α competent cells (C2987H,
617 NEB—New England BioLabs Inc., Ipswich, USA) as a host.
618 **Phage isolation and purification**
619 Phages were isolated from environmental sources through enrichment process[70]. Briefly, 3-4
620 batches of raw sewage were combined in a flask, totalling up to 100 mL, followed by addition
621 of 10 mL of 10× LB along with supplements of 1 mM $CaCl_2$ and $MgCl_2$. Next, 1 mL of
622 overnight cultures of up to three targeted bacterial hosts strains were added into the mixture
623 and incubated at 37 °C overnight. The resulting lysates were purified through centrifugation,
624 filtration, and chloroform treatment[71]. Phage activity was accessed by spotting 10 µL of lysates
625 onto bacterial lawns on soft agar. When bacterial lysis was observed, we plated serial dilutions
626 of the lysate with the host bacteria using the soft overlay (top) agar method and examined for
627 clear plaques on the bacterial lawn after overnight incubation. For two successive rounds,
628 plaques were individually picked from each plate, resuspended in 500 µL of PBS by vigorous
629 vortexing, and reamplified. Lysates prepared from the purified plaques were quantified in
630 plaque-forming units (PFU) per mL and stored at 4 ºC.

631 **Determination of host range, efficiency of plating, one-step growth curve and adsorption**
632 **assay**
633 Host range was examined by spot assays. We applied 10 µL of phage lysate (≥10^8 PFU/mL)
634 onto a bacterial lawn prepared by mixing 1 mL of bacterial culture with 3 mL of soft agar, and
635 spreading over an LB agar plate. For the initial host range assessment on the host subset (*n* =
636 36), spot assay results were further confirmed for their ability to form plaques, verifying
637 productive infection. For screening in broader sets (*n* = 120 and *n* = 156), the resulting zones
638 were recorded as clear (phage clearing bacteria), hazy (bacteria partially lysed), or no lysis (no
639 activity). Three researchers assessed these results blindly to each other and the phage
640 combinations used (Supplementary Fig 5). Efficiency of plating (EOP) was examined by
641 comparing PFU/mL on the host of interest to PFU/mL on the original isolation host. Phage
642 lysates were serially diluted, mixed with each host and plated using top agar to determine the
643 PFU/mL. For one-step growth curves, bacteria from overnight broth cultures were diluted 1:50
644 in LB and grown until an optical density (OD_{600}) of 0.2 was reached (corresponds to ~10^8
645 CFU/mL) (approximately 2 h). The culture was then infected with phage at a multiplicity of
646 infection (MOI) of 0.1. Phage was allowed to adsorb for 5 min at 37°C with orbital agitation
647 at 190 rpm. The mixture was then pelleted (4,000 × g, 2 min, room temperature), resuspended
648 in fresh, pre-warmed LB broth, and incubated. Samples (100 µL) were collected every 5 or 10
649 mins for 1 h, serially diluted in PBS, and plated for phage quantification. The experiment was
650 repeated in at least three different occasions. Using these data, we calculated the latent period
651 and burst size as described previously[72]. Adsorption assays were performed based on the
652 principles of a one-step growth curve, with some modifications. Phages were mixed with their
653 bacterial hosts at an MOI of 0.1 and samples were taken at 0, 5 and 10 mins. Each sample was
654 immediately diluted 1:10 in PBS and centrifuged to remove adsorbed phages; the supernatant
655 was plated for phage quantification, and calculation of the changes in free phage concentration.
656 **Isolation of phage-resistant mutants**
657 To generate phage-resistant mutants, we followed the broth culture method[35]. First, we
658 incubated phages with their respective isolation host at an MOI of 1 in a 96-well microplate,
659 with a total volume of 200 µL each, in nine replicates. After overnight incubation, we
660 transferred 20 µL of the resulting growth to fresh LB containing 10^6 PFU/mL of phage
661 particles. We repeated this process for three consecutive days.
662 After three days, we purified the resistant bacterial colonies through two rounds of single-
663 colony isolation and confirmed phage-resistance by top agar assays using the phage-resistant

664 mutants and their respective phages, expecting an absence of plaques after incubation.
665 Subsequently, we performed adsorption assays to further confirm phage resistance. Stocks of
666 the verified mutants were stored at –80°C until further experimentation.

667 **Transmission electron microscopy (TEM)**

668 To examine through TEM using negative staining, phage lysates were purified using Vivaspin
669 6 centrifugal concentrators (MWCO 1,000,000 kDa; Merck). The lysate was washed several
670 times with SM buffer (100 mM NaCl, 8 mM MgSO4·7H2O, 50 mM Tris-Cl in water). The
671 cleaned lysate was then applied onto a copper TEM grid (200 mesh, SPI, USA) with a carbon-
672 coated ultrathin formvar film. A 10 µL droplet of phage suspension was placed on the grid, left
673 undisturbed for 30 seconds, and then dried using filter paper. Next, a 10 µl droplet of uranyl
674 acetate water solution (1% w/v) was added to the grid surface and left for 20 seconds. After
675 drying the grid with filter paper, it was examined under TEM (JEM-1400 Plus; Jeol, Japan)
676 operating at an accelerating voltage of 80 kV.

677 **Phage evolution**

678 Exponentially growing bacteria and natural (ancestor) phage were mixed at final
679 concentrations of approximately 2×10^6 CFU/mL and 2×10^5 PFU/mL (MOI 0.1), respectively,
680 in a 96-well microplate with a total volume of 200 µL per well. Incubation followed at 37°C
681 with shaking at 190 rpm for 24 h. Then, we added 0.1 volumes of chloroform to each well, and
682 incubated for ten min with occasional mixing to terminate bacterial activity. We centrifuged
683 the microplate at 4000 ×*g* for ten min to pellet the chloroform and bacterial debris. We then
684 transferred the phage-containing supernatant to the corresponding well of a second microplate
685 containing evolutionarily naïve exponentially growing bacteria. We repeated this process daily
686 for up to ten days.

687 Bacterial growth kinetics curves (bacterial lysis by phage) with ancestral or evolved phages
688 were obtained from sequential OD_{600} readings using a microtiter plate reader (Epoch
689 Microplate spectrophotometer; BioTek, Winooski, VT, USA). We added bacterial cultures at
690 exponential growth to individual wells of a 96-well microtiter plate and mixed them with phage
691 lysate at an MOI of 1. The plate was incubated at 37°C in a microplate reader with continuous
692 shaking and recorded the data every 15 mins for up to 24 h. Phage score was calculated using
693 the bacterial areas under the growth curve (AUC) with and without phage[52,53].

694 $$Phage\ score = \frac{(Average\ AUC_{without\ phage} - Average\ AUC_{with\ phage})}{Average\ AUC_{without\ phage}}$$

695 After choosing the focal day for each evolved phage, we purified a single phage genotype from
696 the population by double single-plaque purification.

697 **Phage stability**

698 To examine the stability of phages on long-term storage, we stored clean phage lysate in PBS
699 in 500 µL volumes in 1.7 mL Axygen® polypropylene microcentrifuge tubes (Corning Life
700 Sciences, USA). These tubes were stored at ambient room temperature (~22 ºC), 37 ºC and 4
701 ºC. To track any change in stability, phage count was performed at the interval of 1, 3, 6 and
702 12 months, spanning up to 30 months.

703 **Bacterial and phage genomics and bioinformatics analysis:**

704 To extract bacterial DNA, we revived the bacteria from frozen stock and prepared overnight
705 cultures. A 1.5 mL of overnight culture was used for DNA extraction using the GenElute™
706 Bacterial Genomic DNA Kit (Sigma-Aldrich, St. Louis, MI, United States) following the
707 manufacturer's protocol. For phages, we treated 1 mL of phage lysate with a concentration of
708 $>10^8$ PFU/mL with DNase (1 mg/mL) and RNase A (12.5 mg/mL) for 2 h at 37 °C, followed
709 by an inactivation for 5 mins at 75 °C. Phage DNA extraction was performed using the Norgen
710 phage DNA kit (Norgen Biotek Corp., Thorold, ON, Canada) following the manufacturer's
711 instructions. For cocktail's (*Entelli-02*) genome, we extracted the genome from the final packed
712 product following the same protocol mentioned above, excluding DNase and RNase treatment.
713 We sent bacterial and phage DNA to Azenta Life Sciences in Suzhou, China for indexing and
714 sequencing on an Illumina HiSeq platform.

715 The raw sequencing reads were trimmed using Trimmomatic v0.39[73], followed by assembly
716 using Unicycler v0.4[74], annotation using Prokka v1.13.1[75], NCBI PGAP[76] and RAST
717 annotation server[77]. Snippy v4.0 was used to identify nucleotide variation and SNPs. Phage
718 genomes were assembled into complete genomes and aligned through pairwise sequence
719 alignment using Pyani(https://huttonics.github.io/pyani/). Complete nucleotide sequences
720 were rearranged to match the start gene position of the phage genome. Phages were assigned
721 to the same genus if they had >95% Average Nucleotide Identity (ANI) with other known
722 phages listed in the International Committee on Taxonomy of Viruses (ICTV) database. Phage
723 genomes were examined against antibiotic resistance and virulence factor databases using the
724 ABRicate tool (v1.0.1), and integrase genes in phage annotations were investigated. To analyse
725 of prophage contamination in *Entelli-02,* prophage sequences on host genome were predicted
726 using VirSorter2[78] and verified manually to exclude falsely categorise or low-quality
727 prophages with less than 5000 bp . The raw reads (fastq) of the *Entelli-02* were mapped with
728 component phages' genomes, respective production hosts and predicted prophages using
729 Bowtie2[79] and Samtools[80] to obtain the ratios of read coverage and relative abundance

730 (normalised coverage per million reads) as an indicator of prophage and host genome
731 contamination.

732 **Complementation assay**

733 We designed primers with suitable cut sites for the restriction enzymes targeting genes of
734 interest (Supplementary Table 3). These primers were used to PCR-amplify the respective
735 genes. Next, we performed two overnight double-digestion reactions at 37°C, employing the
736 restriction enzymes, for each gene of interest and the vector pBBRMCS[69]. The digested
737 products were purified through gel electrophoresis on a 0.7% agarose gel, followed by excision
738 and ligation for 2 hours at room temperature using the Instant Sticky-end Ligase Master Mix
739 (NEB) in accordance with the manufacturer's protocol. The ligated product was then
740 chemically transformed into *E. coli* DH5-α competent cells (NEB) following the company's
741 protocol. The transformed colonies were confirmed on antibiotic selection-LB plates and were
742 subsequent validated through Sanger sequencing. The plasmid containing the desired
743 complement was extracted from the confirmed colonies using GenElute™ Plasmid Miniprep
744 Kit (Sigma-Aldrich). The plasmid containing the required complement was then electroporated
745 into the phage-resistant mutants. To verify the restoration of phage infectivity, we conducted
746 top agar and adsorption assays, with the anticipation of observing plaque formation and virion
747 adsorption.

748 ***In vivo* assays (murine phage therapy)**

749 We employed ECC isolate APO57, known to be permissive to all three phages in cocktail-V1,
750 to establish a mouse infection model and determine the optimal bacterial density required to
751 induce severe septicaemia. For the experiment, the bacterial inocula were prepared from an 18-
752 hour culture, washed with PBS and adjusted to a concentration of $1x10^8$ CFU/mL (~0.2 OD_{600}).
753 We used female 8-week-old BALB/c mice (18-20 g) for these experiments, with each mouse
754 receiving either 1×10^6 or 5×10^6 bacterial cells, mixed with 6% porcine stomach mucin in PBS,
755 for a total volume of 200 µL. Mice (n = 3 per group) were injected intraperitoneally and closely
756 monitored for up to 12 h. When the humane endpoint or 12 hpi, whichever earlier, were
757 reached, blood was collected via cardiac puncture, and a laparotomy was performed to obtain
758 a liver section, right kidney, and spleen. The organs were weighed, homogenized in PBS, and
759 plated to enumerate bacterial and phage counts, which were then normalised by organ weight
760 or blood volume.

761 Following the establishment of the infection model, we proceeded with the phage treatment
762 experiment. In this phase, each mouse group received a dose of 200 µL of 5×10^6 CFU/mL. At

763 1 hpi the treatment group ($n = 6$) received 200 µL of PBS containing 1×10^8 PFU/mL of phage,
764 whereas the control group ($n = 6$) received an equivalent volume of sterile PBS. At the
765 established endpoint, blood and organs were collected for bacterial and phage count.

766 **Phage production**

767 Phage production was completed in two stages. In stage 1, each phage in the cocktail was
768 amplified individually with its respective host in a 1000 mL batch. Here, 50 mL of an overnight
769 culture of the host bacteria was added to 1000 mL LB broth supplemented with 1mM $CaCl_2$
770 and $MgCl_2$. This mixture was allowed to grow for ~2 hours at 37ºC with shaking until reaching
771 an optical density of approximately 0.2 (OD600). At this point, phages were added to the
772 mixture at an MOI of 0.1 and allowed to propagate overnight. Next, the lysate was clarified
773 using sequential depth filters with retention rating of 0.5-5 µm (SUPRAcap 50 Pall® Depth
774 filtration capsule SCO50PDH4, Pall Corporation, Modultechnik GmbH, Germany) and of 0.2-
775 3.5 µm (SCO50PDE2, Pall Corp) to remove bacterial aggregates. Pressure was monitored to
776 ensure it did not exceed 2 bar to maintain filter specifications (with manufacturer's maximum
777 limit rating of 3 bar). The filtered lysate was then sterilized into sealed glass bottles within a
778 biosafety cabinet through a sterilization grade filter with a 0.2 µm removal rating (Supor™
779 Mini Kleenpak™ capsules; KA02EKVP2G; Pall Corp) to ensure complete sterilization of the
780 lysate. In stage 2, we purified and packaged the phages in a separate lab environment that was
781 free from bacterial culturing. We used tangential flow filtration (TFF) with buffer exchange
782 using ÄKTA Flux 6 system (product 29038438; Cytiva, Uppsala, Sweden) equipped with a
783 300 kDa nominal molecular weight cut-off (NMWC) microfiltration hollow fibre cartridge
784 (Model; UFP-300-E-4MA, Cytiva). Briefly, the sterile lysate (~900-1000 mL) was diluted up
785 to 10-fold with 1× PBS and processed through TFF. This process was continued until the lysate
786 lost its yellowish colour, indicating replacement of the bacterial media with the buffer, and was
787 concentrated down to ~150 mL final volume. The lysate was then collected and resterilised
788 using a 0.2 µm filter as mentioned above. After clean-up and verification of the titre, the lysate
789 of each phage was mixed, or diluted in 1× PBS as needed, to obtain a cocktail with a target
790 final phage concentration of $>10^8$ PFU/mL for each phage component. To clean endotoxins
791 from the cocktail, we initially applied an EndoTrap®HD affinity column (Cat no. LET0035;
792 Lionex GmbH, Germany) following the manufacturer's instruction. However, the endotoxin
793 level remained above the acceptable threshold. We therefore performed a 1-Octanol
794 purification[71]. The endotoxin concentration at different stages of the purification process was
795 assessed using the EndoZyme® II (Lot 22599; Hyglos GmbH (bioMérieux) Germany) and

796 Endosafe® PTS™ cartridges (Product: PTS20F, Charles River Laboratories, MA, USA) kits.
797 Once a satisfactory endotoxin level was achieved, the preparation was again filter sterilised
798 and packed in 35 mL batches in sealed sterile glass vials (FILL-EASE™ Cat no. SV-50C02
799 Huayi Isotopes Company (Jiangsu, China) with syringe access. The vails were labelled and
800 stored at 4 ºC for clinical use. Third-party independent validation for sterility (US
801 Pharmacopeia; USP 71) and endotoxin (USP 85) for each production batch was performed by
802 Eurofins BioPharma Product Testing in Sydney, Australia. Phage titration was performed to
803 verify the phage recovery throughout the process and product stability during storage.
804
805 **Statistical analysis:** The statistical analysis was performed using R 4.2.3 and GraphPad Prism
806 v9.1. Mean and standard error of mean, median, percentage and area under curve were
807 calculated as appropriate, and statistical tests were performed accordingly and reported in
808 figures where appropriate. Two-sided *p*-values were calculated and reported where applicable.
809 The cut-off for the phage score was calculated using maximum likelihood estimation based on
810 receiver operating characteristic curve implemented online[55] (Supplementary Fig 14). Graphs
811 were drawn using ggplot2 in R and Figures were drawn using Inkscape and Biorender.
812
813 **Ethical statement:** All protocols involving animals were reviewed and approved by the
814 Monash University Animal Ethics Committee (Project ID: 2022-27681-80733) and the animals
815 were housed at the Monash Animal Research Facility, Monash University. We received all the
816 bacterial isolates from the Department of Infectious Diseases at the Alfred Hospital without
817 identifiable patient data. We conducted all procedures in strict adherence to institutional
818 guidelines.
819
820 **Data availability (key resources table, lead contact, materials availability, data and code**
821 **availability):**
822 All data (supplementary data and figures) and results that were generated during this study
823 are deposited at https://github.com/ECCphage.
824 Additional data are available in the Article, Online methods and Supplementary
825 data/figure/table.
826 Genome sequences generated during this study are deposited at NCBI database under project
827 ID PRJNA629076.
828

829 ## Acknowledgements

830 The authors thank Professor Jian Li Monash University for providing plasmids used in this
831 study, Associate Professor David McCarthy for raw sewage samples for phage isolation,

researchers Leo Kan and Natasha Smith for their help in blind interpretation of spot assay results. We acknowledge Monash Animal Research Facility (MARP) for providing the necessary facilities for animal experiments; MASSIVE HPC facility (www.massive.org.au) for providing us with cluster time for data analysis and Monash Ramaciotti Cryo-EM platform for the use of facilities.

This work, including the efforts of Jeremy J. Barr, was funded by the National Health and Medical Research Council (NHMRC: 1156588 and 2026130).

Author contributions

D.S, A.Y.P. and J.J.B. conceived the study. D.S, F.G.A. and A.P. performed phage isolation. D.S. performed phenotypic and genotypic characterization of phages, including all bioinformatics. D.S. and R.P. planned and performed complementation experiments. D.S. and R.D. performed phage evolution experiments. D.S. performed animal experiment, with help from F.G.A. (pilot study) and X.K. (pilot study). F.G.A. and L.B. performed spot assay and growth kinetics in the Alfred Hospital. N.M. provided strain information. D.K. performed TEM. J.J.B. and A.Y.P. supervised the project. J.J.B. funded the project. D.S. and J.J.B. wrote the original draft. All authors were involved in reviewing and editing the final manuscript.

Lead contact: Jeremy Barr and Dinesh Subedi

References

1. World Health Organization. Addressing the burden of infections and antimicrobial resistance associated with health care focus on G7 countries. (ed. Aaes-Jorgensen, A.) (WHO, Geneva, Addressing the burden of infections and antimicrobial resistance associated with health care focus on G7 countries 2022).
2. Gordillo Altamirano, F.L. & Barr, J.J. Phage Therapy in the Postantibiotic Era. *Clinical microbiology reviews* **32**(2019).
3. Abedon, S.T., Kuhl, S.J., Blasdel, B.G. & Kutter, E.M. Phage treatment of human infections. *Bacteriophage* **1**, 66-85 (2011).
4. Chan, B.K., Abedon, S.T. & Loc-Carrillo, C. Phage cocktails and the future of phage therapy. *Future Microbiol* **8**, 769-783 (2013).
5. Blasco, L.*, et al.* Case report: Analysis of phage therapy failure in a patient with a Pseudomonas aeruginosa prosthetic vascular graft infection. *Front Med (Lausanne)* **10**, 1199657 (2023).
6. Petrovic Fabijan, A., Iredell, J., Danis-Wlodarczyk, K., Kebriaei, R. & Abedon, S.T. Translating phage therapy into the clinic: Recent accomplishments but continuing challenges. *PLoS Biol* **21**, e3002119 (2023).
7. Pires, D.P., Costa, A.R., Pinto, G., Meneses, L. & Azeredo, J. Current challenges and future opportunities of phage therapy. *FEMS Microbiol Rev* **44**, 684-700 (2020).

872 8. Uyttebroek, S.*, et al.* Safety and efficacy of phage therapy in difficult-to-treat
873 infections: a systematic review. *The Lancet. Infectious diseases* **22**, e208-e220 (2022).
874 9. Rhoads, D.D.*, et al.* Bacteriophage therapy of venous leg ulcers in humans: results of
875 a phase I safety trial. *J Wound Care* **18**, 237-238, 240-233 (2009).
876 10. Wright, A., Hawkins, C.H., Anggard, E.E. & Harper, D.R. A controlled clinical trial of a
877 therapeutic bacteriophage preparation in chronic otitis due to antibiotic-resistant
878 Pseudomonas aeruginosa; a preliminary report of efficacy. *Clinical otolaryngology :*
879 *official journal of ENT-UK ; official journal of Netherlands Society for Oto-Rhino-*
880 *Laryngology & Cervico-Facial Surgery* **34**, 349-357 (2009).
881 11. Jault, P.*, et al.* Efficacy and tolerability of a cocktail of bacteriophages to treat burn
882 wounds infected by Pseudomonas aeruginosa (PhagoBurn): a randomised,
883 controlled, double-blind phase 1/2 trial. *The Lancet. Infectious diseases* **19**, 35-45
884 (2019).
885 12. Sarker, S.A.*, et al.* Oral application of Escherichia coli bacteriophage: safety tests in
886 healthy and diarrheal children from Bangladesh. *Environ Microbiol* **19**, 237-250
887 (2017).
888 13. Pirnay, J.P. & Verbeken, G. Magistral Phage Preparations: Is This the Model for
889 Everyone? *Clinical infectious diseases : an official publication of the Infectious*
890 *Diseases Society of America* **77**, S360-S369 (2023).
891 14. Pirnay, J.P.*, et al.* The phage therapy paradigm: prêt-à-porter or sur-mesure?
892 *Pharmaceutical research* **28**, 934-937 (2011).
893 15. Jean-Paul, P.*, et al.* Retrospective, observational analysis of the first one hundred
894 consecutive cases of personalized bacteriophage therapy of difficult-to-treat
895 infections facilitated by a Belgian consortium. *medRxiv*, 2023.2008.2028.23294728
896 (2023).
897 16. Rice, L.B. Federal funding for the study of antimicrobial resistance in nosocomial
898 pathogens: no ESKAPE. *The Journal of infectious diseases* **197**, 1079-1081 (2008).
899 17. Mulani, M.S., Kamble, E.E., Kumkar, S.N., Tawre, M.S. & Pardesi, K.R. Emerging
900 Strategies to Combat ESKAPE Pathogens in the Era of Antimicrobial Resistance: A
901 Review. *Frontiers in microbiology* **10**, 539-539 (2019).
902 18. Iredell, J., Brown, J. & Tagg, K. Antibiotic resistance in Enterobacteriaceae:
903 mechanisms and clinical implications. *Bmj* **352**, h6420 (2016).
904 19. Roberts, L.W.*, et al.* Genomic analysis of carbapenemase-producing
905 Enterobacteriaceae in Queensland reveals widespread transmission of bla IMP-4 on
906 an IncHI2 plasmid. *Microb Genom* **6**(2020).
907 20. Roberts, L.W.*, et al.* Integrating multiple genomic technologies to investigate an
908 outbreak of carbapenemase-producing Enterobacter hormaechei. *Nat Commun* **11**,
909 466 (2020).
910 21. Lydeamore, M.J.*, et al.* Burden of five healthcare associated infections in Australia.
911 *Antimicrob Resist Infect Control* **11**, 69 (2022).
912 22. Annavajhala, M.K., Gomez-Simmonds, A. & Uhlemann, A.C. Multidrug-Resistant
913 Enterobacter cloacae Complex Emerging as a Global, Diversifying Threat. *Frontiers in*
914 *microbiology* **10**, 44 (2019).
915 23. Lane, C.R.*, et al.* Search and Contain: Impact of an Integrated Genomic and
916 Epidemiological Surveillance and Response Program for Control of Carbapenemase-
917 producing Enterobacterales. *Clinical infectious diseases : an official publication of the*
918 *Infectious Diseases Society of America* **73**, e3912-e3920 (2021).

24. Davin-Regli, A., Lavigne, J.-P. & Pagès, J.-M. Enterobacter spp.: Update on taxonomy, clinical aspects, and emerging antimicrobial resistance. *Clinical microbiology reviews* **32**, e00002-00019 (2019).
25. Aleidan, F.A.S.*, et al.* Incidence and risk factors of carbapenem-resistant Enterobacteriaceae infection in intensive care units: a matched case-control study. *Expert Rev Anti Infect Ther* **19**, 393-398 (2021).
26. Peirano, G.*, et al.* Genomic Epidemiology of Global Carbapenemase-Producing Enterobacter spp., 2008-2014. *Emerging infectious diseases* **24**, 1010-1019 (2018).
27. Murray, C.J.*, et al.* Global burden of bacterial antimicrobial resistance in 2019: a systematic analysis. *The Lancet* **399**, 629-655 (2022).
28. Flynn, E., Papanicolas, L.E., Anagnostou, N., Warner, M.S. & Rogers, G.B. Carbapenemase-producing Enterobacterales: a profound threat to Australian public health. *The Medical journal of Australia* **219**, 290-292 (2023).
29. Macesic, N.*, et al.* Genomic dissection of endemic carbapenem resistance reveals metallo-beta-lactamase dissemination through clonal, plasmid and integron transfer. *Nat Commun* **14**, 4764 (2023).
30. Walker, P.J.*, et al.* Recent changes to virus taxonomy ratified by the International Committee on Taxonomy of Viruses (2022). *Archives of virology* **167**, 2429-2440 (2022).
31. Kutter, E. Phage host range and efficiency of plating. *Methods Mol Biol* **501**, 141-149 (2009).
32. Jonczyk-Matysiak, E.*, et al.* Factors determining phage stability/activity: challenges in practical phage application. *Expert Rev Anti Infect Ther* **17**, 583-606 (2019).
33. Xu, Z.*, et al.* Shelf-life prediction and storage stability of Aeromonas bacteriophage vB_AsM_ZHF. *Virus research* **323**, 198997 (2022).
34. Wright, R.C.T., Friman, V.P., Smith, M.C.M. & Brockhurst, M.A. Functional diversity increases the efficacy of phage combinations. *Microbiology (Reading)* **167**(2021).
35. Wright, R.C.T., Friman, V.P., Smith, M.C.M. & Brockhurst, M.A. Resistance Evolution against Phage Combinations Depends on the Timing and Order of Exposure. *mBio* **10**(2019).
36. Gordillo Altamirano, F.*, et al.* Bacteriophage-resistant Acinetobacter baumannii are resensitized to antimicrobials. *Nat Microbiol* **6**, 157-161 (2021).
37. Samuel, G. & Reeves, P. Biosynthesis of O-antigens: genes and pathways involved in nucleotide sugar precursor synthesis and O-antigen assembly. *Carbohydr Res* **338**, 2503-2519 (2003).
38. Heller, K. & Braun, V. Polymannose O-antigens of Escherichia coli, the binding sites for the reversible adsorption of bacteriophage T5+ via the L-shaped tail fibers. *J Virol* **41**, 222-227 (1982).
39. Romeyer Dherbey, J., Parab, L., Gallie, J. & Bertels, F. Stepwise Evolution of E. coli C and PhiX174 Reveals Unexpected Lipopolysaccharide (LPS) Diversity. *Mol Biol Evol* **40**(2023).
40. Shin, H.*, et al.* Receptor diversity and host interaction of bacteriophages infecting Salmonella enterica serovar Typhimurium. *PloS one* **7**, e43392 (2012).
41. Xu, D.*, et al.* Outer membrane protein OmpW is the receptor for typing phage VP5 in the Vibrio cholerae O1 El Tor biotype. *J Virol* **88**, 7109-7111 (2014).
42. Wu, X.B.*, et al.* Outer membrane protein OmpW of Escherichia coli is required for resistance to phagocytosis. *Res Microbiol* **164**, 848-855 (2013).

966 43. Pilsl, H., Smajs, D. & Braun, V. Characterization of colicin S4 and its receptor, OmpW,
967 a minor protein of the Escherichia coli outer membrane. *Journal of bacteriology* **181**,
968 3578-3581 (1999).
969 44. Pagnout, C.*, et al.* Pleiotropic effects of rfa-gene mutations on Escherichia coli
970 envelope properties. *Scientific reports* **9**, 9696 (2019).
971 45. Cote, J.M. & Taylor, E.A. The Glycosyltransferases of LPS Core: A Review of Four
972 Heptosyltransferase Enzymes in Context. *Int J Mol Sci* **18**(2017).
973 46. Meyer, C., Hoffmann, C., Haas, R. & Schubert, S. The role of the galU gene of
974 uropathogenic Escherichia coli in modulating macrophage TNF-alpha response. *Int J*
975 *Med Microbiol* **305**, 893-901 (2015).
976 47. Wang, X. & Quinn, P.J. Lipopolysaccharide: Biosynthetic pathway and structure
977 modification. *Prog Lipid Res* **49**, 97-107 (2010).
978 48. Abedon, S.T. Lysis from without. *Bacteriophage* **1**, 46-49 (2011).
979 49. Friman, V.P.*, et al.* Pre-adapting parasitic phages to a pathogen leads to increased
980 pathogen clearance and lowered resistance evolution with Pseudomonas aeruginosa
981 cystic fibrosis bacterial isolates. *J Evol Biol* **29**, 188-198 (2016).
982 50. Meyer, J.R.*, et al.* Repeatability and contingency in the evolution of a key innovation
983 in phage lambda. *Science* **335**, 428-432 (2012).
984 51. Borin, J.M., Avrani, S., Barrick, J.E., Petrie, K.L. & Meyer, J.R. Coevolutionary phage
985 training leads to greater bacterial suppression and delays the evolution of phage
986 resistance. *Proceedings of the National Academy of Sciences of the United States of*
987 *America* **118**(2021).
988 52. Konopacki, M., Grygorcewicz, B., Dołęgowska, B., Kordas, M. & Rakoczy, R.
989 PhageScore: A simple method for comparative evaluation of bacteriophages lytic
990 activity. *Biochemical Engineering Journal* **161**, 107652 (2020).
991 53. Xie, Y., Wahab, L. & Gill, J.J. Development and Validation of a Microtiter Plate-Based
992 Assay for Determination of Bacteriophage Host Range and Virulence. *Viruses*
993 **10**(2018).
994 54. Guo, H.*, et al.* Molecular analysis of the O-antigen gene cluster of Escherichia coli
995 O86:B7 and characterization of the chain length determinant gene (wzz). *Appl*
996 *Environ Microbiol* **71**, 7995-8001 (2005).
997 55. Goksuluk, D., Korkmaz, S. & Zararsiz, G. easyROC: an interactive web-tool for ROC
998 curve analysis using R language environment.
999 56. Daneshian, M., Guenther, A., Wendel, A., Hartung, T. & von Aulock, S. In vitro
1000 pyrogen test for toxic or immunomodulatory drugs. *J Immunol Methods* **313**, 169-
1001 175 (2006).
1002 57. Aslam, S.*, et al.* Lessons Learned From the First 10 Consecutive Cases of Intravenous
1003 Bacteriophage Therapy to Treat Multidrug-Resistant Bacterial Infections at a Single
1004 Center in the United States. *Open Forum Infect Dis* **7**, ofaa389 (2020).
1005 58. Gordillo Altamirano, F.L. & Barr, J.J. Unlocking the next generation of phage therapy:
1006 the key is in the receptors. *Curr Opin Biotechnol* **68**, 115-123 (2021).
1007 59. Kortright, K.E., Chan, B.K., Koff, J.L. & Turner, P.E. Phage Therapy: A Renewed
1008 Approach to Combat Antibiotic-Resistant Bacteria. *Cell host & microbe* **25**, 219-232
1009 (2019).
1010 60. Merabishvili, M., Pirnay, J.P. & De Vos, D. Guidelines to Compose an Ideal
1011 Bacteriophage Cocktail. *Methods Mol Biol* **1693**, 99-110 (2018).

1012 61. Suh, G.A.*, et al.* Considerations for the Use of Phage Therapy in Clinical Practice.
1013 *Antimicrobial agents and chemotherapy* **66**, e0207121 (2022).
1014 62. Betts, A., Vasse, M., Kaltz, O. & Hochberg, M.E. Back to the future: evolving
1015 bacteriophages to increase their effectiveness against the pathogen Pseudomonas
1016 aeruginosa PAO1. *Evol Appl* **6**, 1054-1063 (2013).
1017 63. Khan Mirzaei, M. & Nilsson, A.S. Isolation of phages for phage therapy: a comparison
1018 of spot tests and efficiency of plating analyses for determination of host range and
1019 efficacy. *PloS one* **10**, e0118557 (2015).
1020 64. Holtappels, D., Alfenas-Zerbini, P. & Koskella, B. Drivers and consequences of
1021 bacteriophage host range. *FEMS Microbiol Rev* **47**(2023).
1022 65. Williams, H.T. Phage-induced diversification improves host evolvability. *BMC Evol*
1023 *Biol* **13**, 17 (2013).
1024 66. Woolhouse, M.E., Webster, J.P., Domingo, E., Charlesworth, B. & Levin, B.R.
1025 Biological and biomedical implications of the co-evolution of pathogens and their
1026 hosts. *Nature genetics* **32**, 569-577 (2002).
1027 67. Paterson, S.*, et al.* Antagonistic coevolution accelerates molecular evolution. *Nature*
1028 **464**, 275-278 (2010).
1029 68. Knirel, Y.A.*, et al.* Variations in O-antigen biosynthesis and O-acetylation associated
1030 with altered phage sensitivity in Escherichia coli 4s. *Journal of bacteriology* **197**, 905-
1031 912 (2015).
1032 69. Kovach, M.E.*, et al.* Four new derivatives of the broad-host-range cloning vector
1033 pBBR1MCS, carrying different antibiotic-resistance cassettes. *Gene* **166**, 175-176
1034 (1995).
1035 70. Van Twest, R. & Kropinski, A.M. Bacteriophage enrichment from water and soil.
1036 *Methods Mol Biol* **501**, 15-21 (2009).
1037 71. Bonilla, N.*, et al.* Phage on tap-a quick and efficient protocol for the preparation of
1038 bacteriophage laboratory stocks. *PeerJ* **4**, e2261 (2016).
1039 72. Ellis, E.L. & Delbruck, M. The growth of bacteriophage. *J Gen Physiol* **22**, 365-384
1040 (1939).
1041 73. Bolger, A.M., Lohse, M. & Usadel, B. Trimmomatic: a flexible trimmer for Illumina
1042 sequence data. *Bioinformatics (Oxford, England)* **30**, 2114-2120 (2014).
1043 74. Wick, R.R., Judd, L.M., Gorrie, C.L. & Holt, K.E. Unicycler: resolving bacterial genome
1044 assemblies from short and long sequencing reads. *PLoS computational biology* **13**,
1045 e1005595 (2017).
1046 75. Seemann, T. Prokka: rapid prokaryotic genome annotation. *Bioinformatics (Oxford,*
1047 *England)* **30**, 2068-2069 (2014).
1048 76. Tatusova, T.*, et al.* NCBI prokaryotic genome annotation pipeline. *Nucleic acids*
1049 *research* **44**, 6614-6624 (2016).
1050 77. Aziz, R.K.*, et al.* The RAST Server: rapid annotations using subsystems technology.
1051 *BMC genomics* **9**, 75 (2008).
1052 78. Roux, S., Enault, F., Hurwitz, B.L. & Sullivan, M.B. VirSorter: mining viral signal from
1053 microbial genomic data. *PeerJ* **3**, e985 (2015).
1054 79. Langmead, B. & Salzberg, S.L. Fast gapped-read alignment with Bowtie 2. *Nat*
1055 *Methods* **9**, 357-359 (2012).
1056 80. Li, H.*, et al.* The Sequence Alignment/Map format and SAMtools. *Bioinformatics*
1057 *(Oxford, England)* **25**, 2078-2079 (2009).
1058

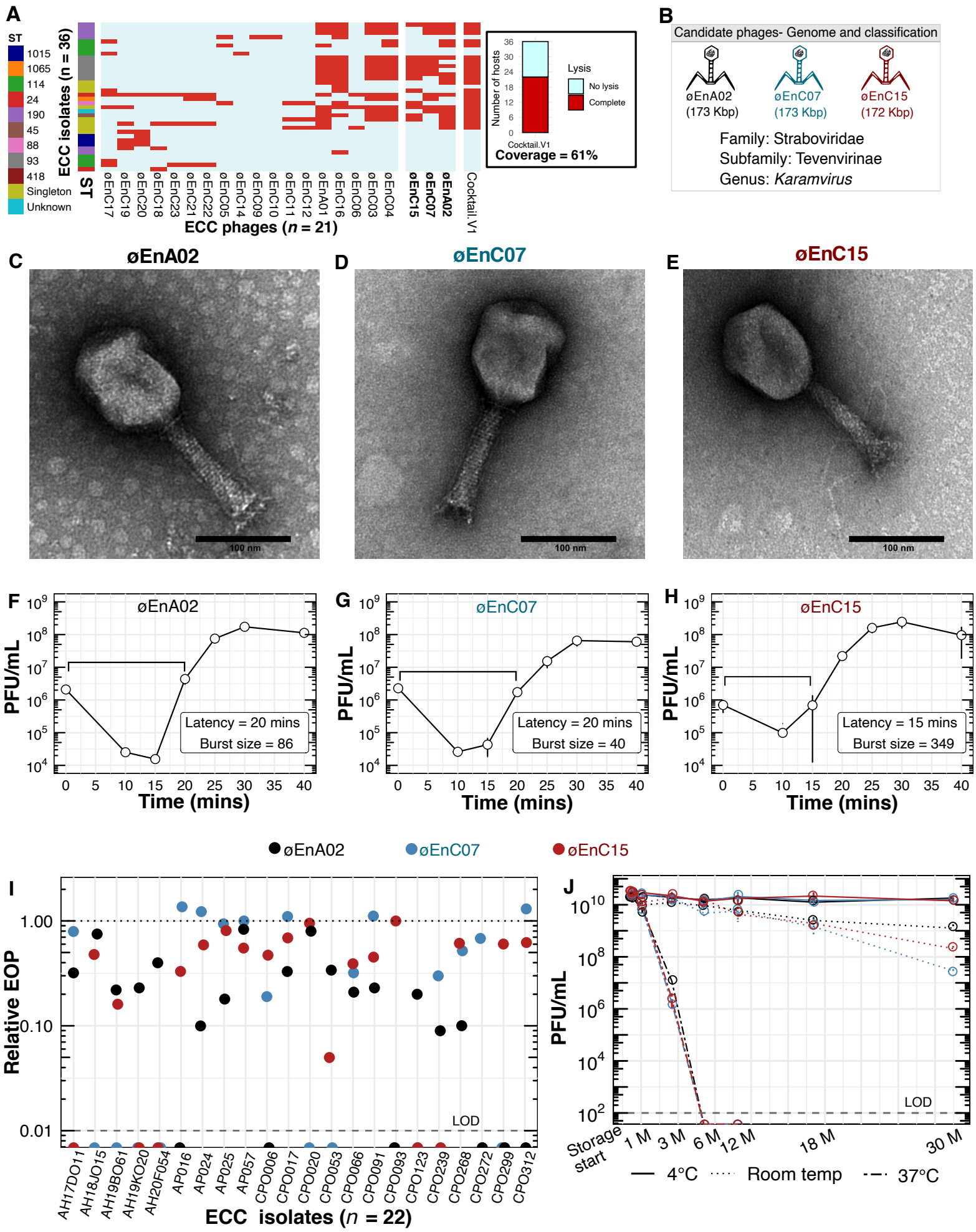
A
ST
1015
1065
114
24
190
45
88
93
418
Singleton
Unknown
ECC isolates (n = 36)
ST
øEnC17
øEnC19
øEnC20
øEnC18
øEnC23
øEnC21
øEnC22
øEnC05
øEnC14
øEnC09
øEnC10
øEnC11
øEnC12
øEnA01
øEnC16
øEnC06
øEnC03
øEnC04
øEnC15
øEnC07
øEnA02
Cocktail.V1
ECC phages (n = 21)
Number of hosts
Lysis
No lysis
Complete
Cocktail.V1
Coverage = 61%
B
Candidate phages- Genome and classification
øEnA02
(173 Kbp)
øEnC07
(173 Kbp)
øEnC15
(172 Kbp)
Family: Straboviridae
Subfamily: Tevenvirinae
Genus: Karamvirus
C
øEnA02
D
øEnC07
E
øEnC15
100 nm
F
øEnA02
Latency = 20 mins
Burst size = 86
G
øEnC07
Latency = 20 mins
Burst size = 40
H
øEnC15
Latency = 15 mins
Burst size = 349
PFU/mL
Time (mins)
øEnA02
øEnC07
øEnC15
I
Relative EOP
LOD
AH17DO11
AH18JO15
AH19BO61
AH19KO20
AH20F054
AP016
AP024
AP025
AP057
CPO006
CPO017
CPO020
CPO053
CPO066
CPO091
CPO093
CPO123
CPO239
CPO268
CPO272
CPO299
CPO312
ECC isolates (n = 22)
J
PFU/mL
LOD
Storage start
1 M
3 M
6 M
12 M
18 M
30 M
4°C
Room temp
37°C

Fig 1

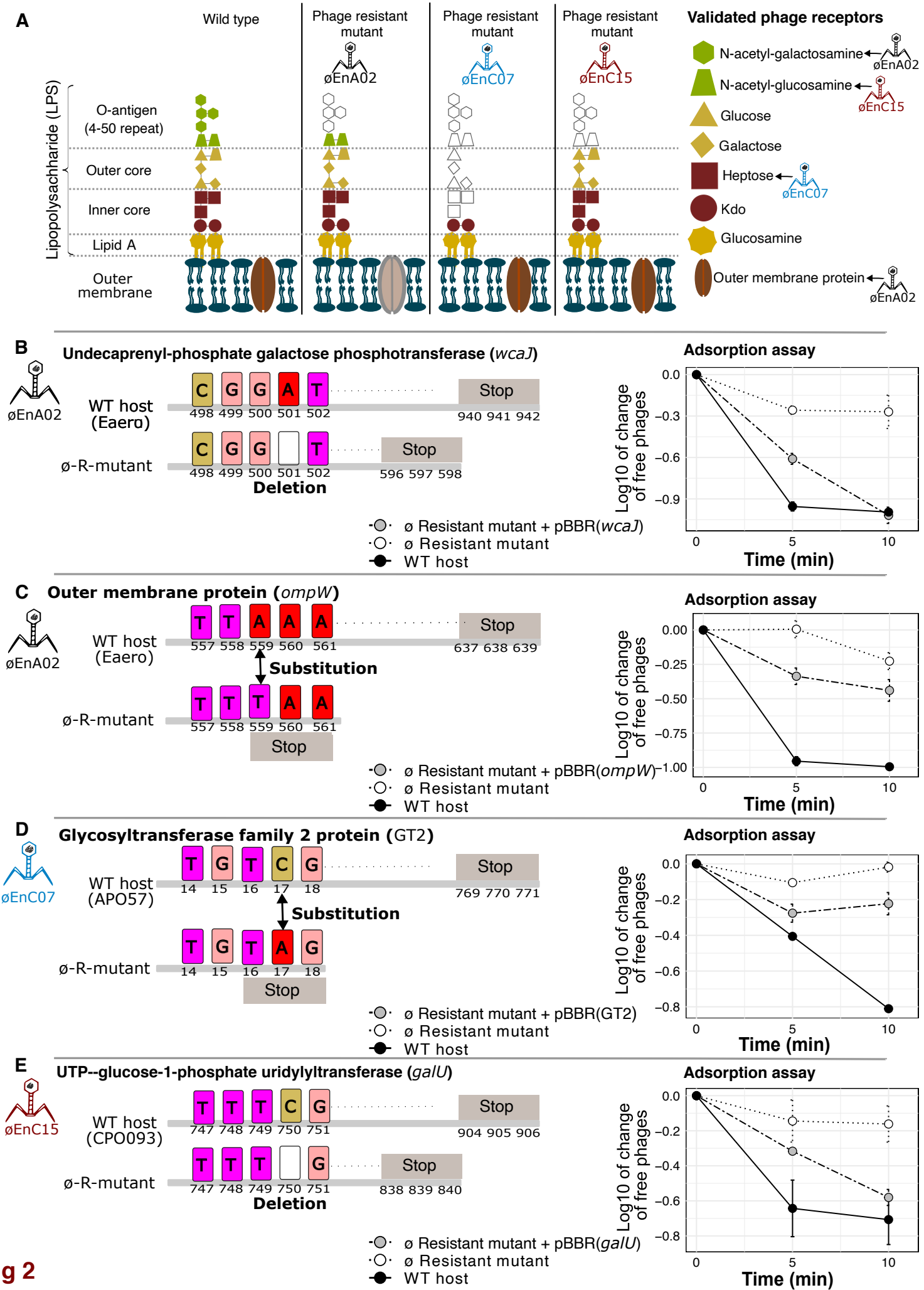
A
Wild type
Phage resistant mutant
øEnA02
Phage resistant mutant
øEnC07
Phage resistant mutant
øEnC15
Validated phage receptors
N-acetyl-galactosamine
øEnA02
N-acetyl-glucosamine
øEnC15
Glucose
Galactose
Heptose
øEnC07
Kdo
Glucosamine
Outer membrane protein
øEnA02
Lipopolysachharide (LPS)
O-antigen (4-50 repeat)
Outer core
Inner core
Lipid A
Outer membrane
B
Undecaprenyl-phosphate galactose phosphotransferase (wcaJ)
øEnA02
WT host (Eaero)
C G G A T
498 499 500 501 502
Stop
940 941 942
ø-R-mutant
C G G T
498 499 500 501 502
Stop
596 597 598
Deletion
Adsorption assay
Log10 of change of free phages
0.0
−0.3
−0.6
−0.9
0
5
10
Time (min)
ø Resistant mutant + pBBR(wcaJ)
ø Resistant mutant
WT host
C
Outer membrane protein (ompW)
øEnA02
WT host (Eaero)
T T A A A
557 558 559 560 561
Stop
637 638 639
Substitution
ø-R-mutant
T T T A A
557 558 559 560 561
Stop
Adsorption assay
Log10 of change of free phages
0.00
−0.25
−0.50
−0.75
−1.00
0
5
10
Time (min)
ø Resistant mutant + pBBR(ompW)
ø Resistant mutant
WT host
D
Glycosyltransferase family 2 protein (GT2)
øEnC07
WT host (APO57)
T G T C G
14 15 16 17 18
Stop
769 770 771
Substitution
ø-R-mutant
T G T A G
14 15 16 17 18
Stop
Adsorption assay
Log10 of change of free phages
0.0
−0.2
−0.4
−0.6
−0.8
0
5
10
Time (min)
ø Resistant mutant + pBBR(GT2)
ø Resistant mutant
WT host
E
UTP--glucose-1-phosphate uridylyltransferase (galU)
øEnC15
WT host (CPO093)
T T T C G
747 748 749 750 751
Stop
904 905 906
ø-R-mutant
T T T G
747 748 749 750 751
Stop
838 839 840
Deletion
Adsorption assay
Log10 of change of free phages
0.0
−0.2
−0.4
−0.6
−0.8
0
5
10
Time (min)
ø Resistant mutant + pBBR(galU)
ø Resistant mutant
WT host

Fig 2

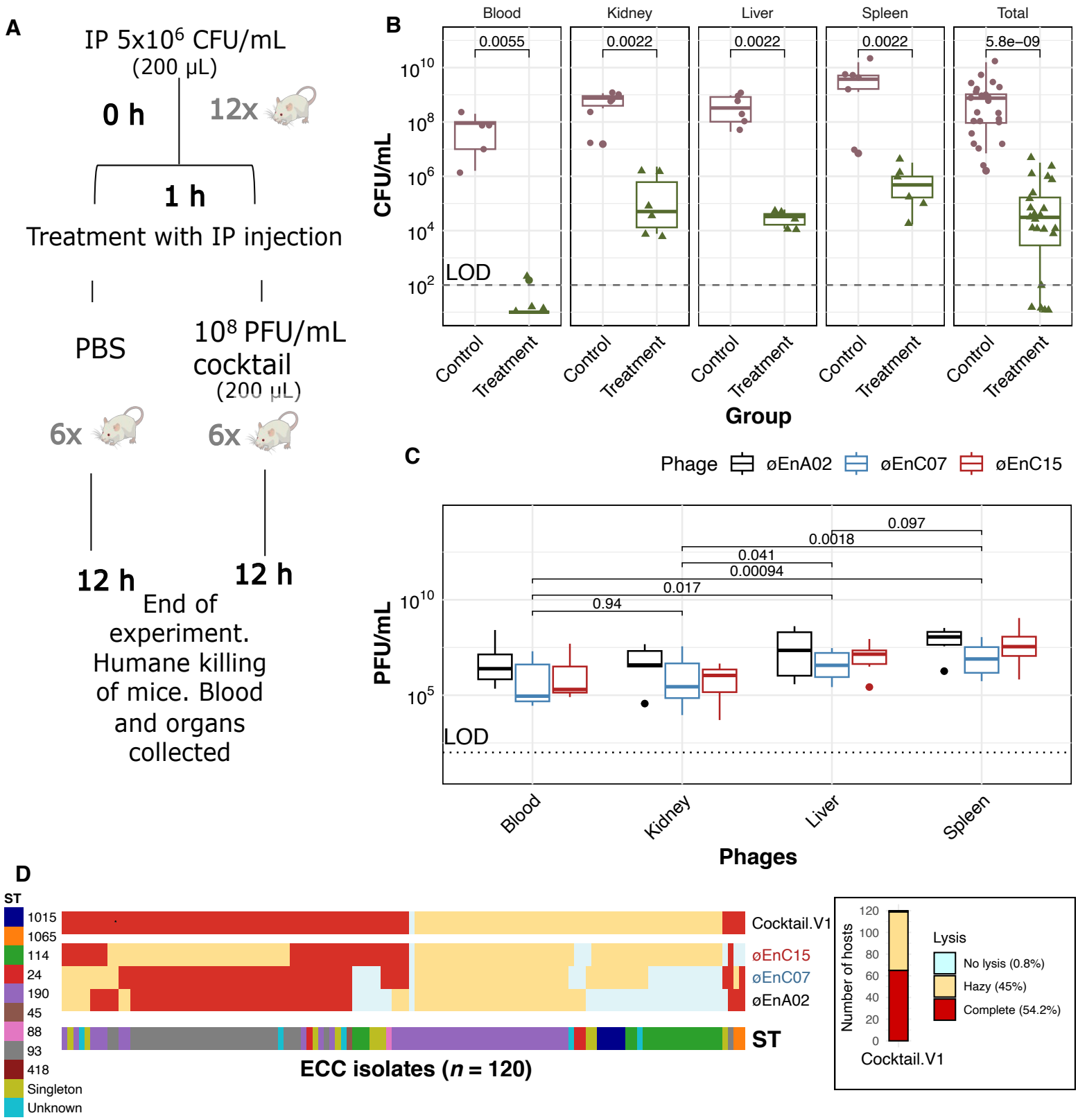
A
IP 5x10^6 CFU/mL
(200 µL)
0 h
12x
1 h
Treatment with IP injection
PBS
10^8 PFU/mL
cocktail
(200 µL)
6x
6x
12 h
12 h
End of experiment. Humane killing of mice. Blood and organs collected
B
Blood
Kidney
Liver
Spleen
Total
0.0055
0.0022
0.0022
0.0022
5.8e−09
CFU/mL
LOD
Control
Treatment
Group
C
Phage
øEnA02
øEnC07
øEnC15
0.097
0.0018
0.041
0.00094
0.017
0.94
PFU/mL
LOD
Blood
Kidney
Liver
Spleen
Phages
D
ST
1015
1065
114
24
190
45
88
93
418
Singleton
Unknown
Cocktail.V1
øEnC15
øEnC07
øEnA02
ST
ECC isolates (n = 120)
Number of hosts
Lysis
No lysis (0.8%)
Hazy (45%)
Complete (54.2%)
Cocktail.V1

Fig 3

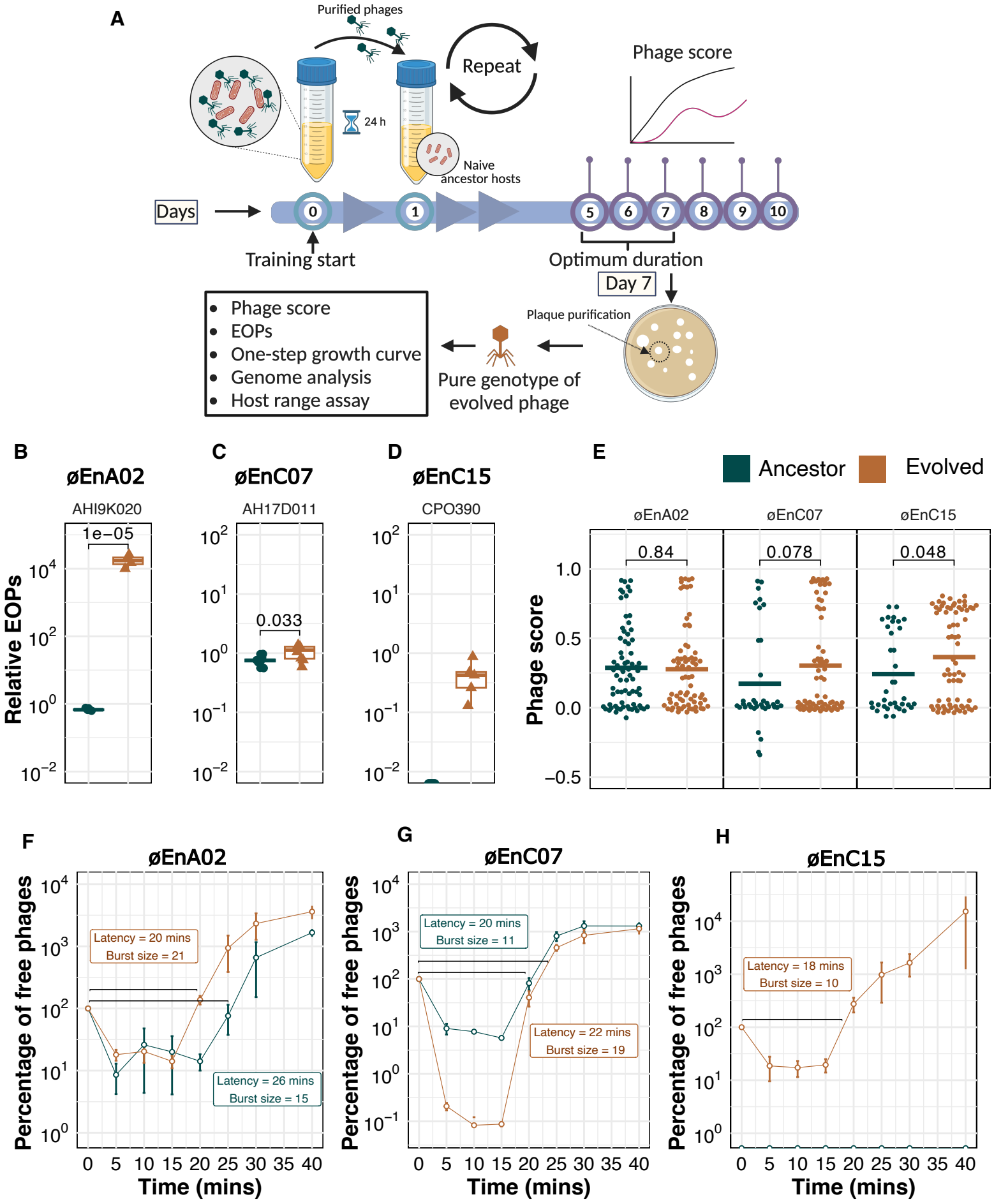
A
Purified phages
Repeat
24 h
Naive ancestor hosts
Phage score
Days
0
1
5
6
7
8
9
10
Training start
Optimum duration
Day 7
Plaque purification
Pure genotype of evolved phage
Phage score
EOPs
One-step growth curve
Genome analysis
Host range assay
B
øEnA02
AHI9K020
1e−05
Relative EOPs
C
øEnC07
AH17D011
0.033
D
øEnC15
CPO390
E
Ancestor
Evolved
øEnA02
øEnC07
øEnC15
0.84
0.078
0.048
Phage score
F
øEnA02
Latency = 20 mins
Burst size = 21
Latency = 26 mins
Burst size = 15
Percentage of free phages
Time (mins)
G
øEnC07
Latency = 20 mins
Burst size = 11
Latency = 22 mins
Burst size = 19
H
øEnC15
Latency = 18 mins
Burst size = 10

Fig 4

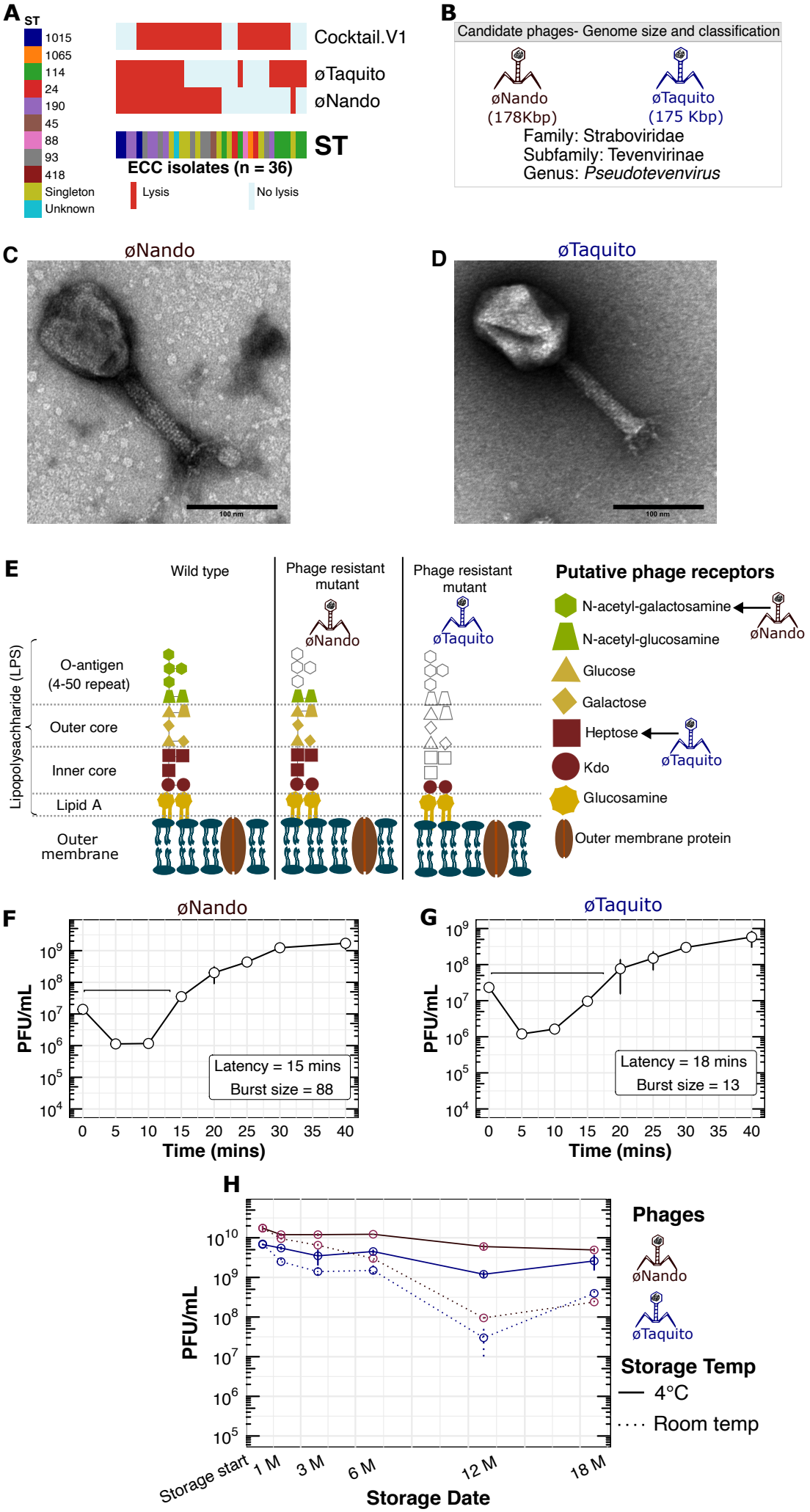
A
ST
1015
1065
114
24
190
45
88
93
418
Singleton
Unknown
Cocktail.V1
øTaquito
øNando
ST
ECC isolates (n = 36)
Lysis
No lysis
B
Candidate phages- Genome size and classification
øNando
(178Kbp)
øTaquito
(175 Kbp)
Family: Straboviridae
Subfamily: Tevenvirinae
Genus: Pseudotevenvirus
C
øNando
100 nm
D
øTaquito
100 nm
E
Wild type
Phage resistant mutant
Phage resistant mutant
øNando
øTaquito
Putative phage receptors
N-acetyl-galactosamine
N-acetyl-glucosamine
Glucose
Galactose
Heptose
Kdo
Glucosamine
Outer membrane protein
Lipopolysachharide (LPS)
O-antigen
(4-50 repeat)
Outer core
Inner core
Lipid A
Outer membrane
F
øNando
PFU/mL
Latency = 15 mins
Burst size = 88
Time (mins)
G
øTaquito
PFU/mL
Latency = 18 mins
Burst size = 13
Time (mins)
H
PFU/mL
Phages
øNando
øTaquito
Storage Temp
4°C
Room temp
Storage start
1 M
3 M
6 M
12 M
18 M
Storage Date

Fig 5

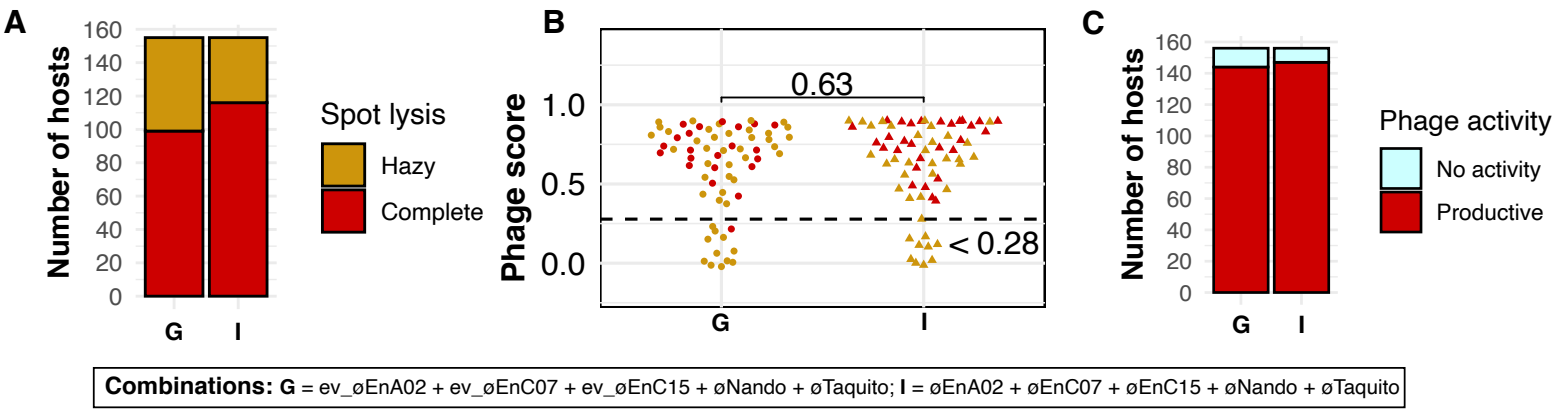
A
Number of hosts
160
140
120
100
80
60
40
20
0
G
I
Spot lysis
Hazy
Complete
B
Phage score
1.0
0.5
0.0
0.63
< 0.28
G
I
C
Number of hosts
Phage activity
No activity
Productive
G
I
Combinations: G = ev_øEnA02 + ev_øEnC07 + ev_øEnC15 + øNando + øTaquito; I = øEnA02 + øEnC07 + øEnC15 + øNando + øTaquito

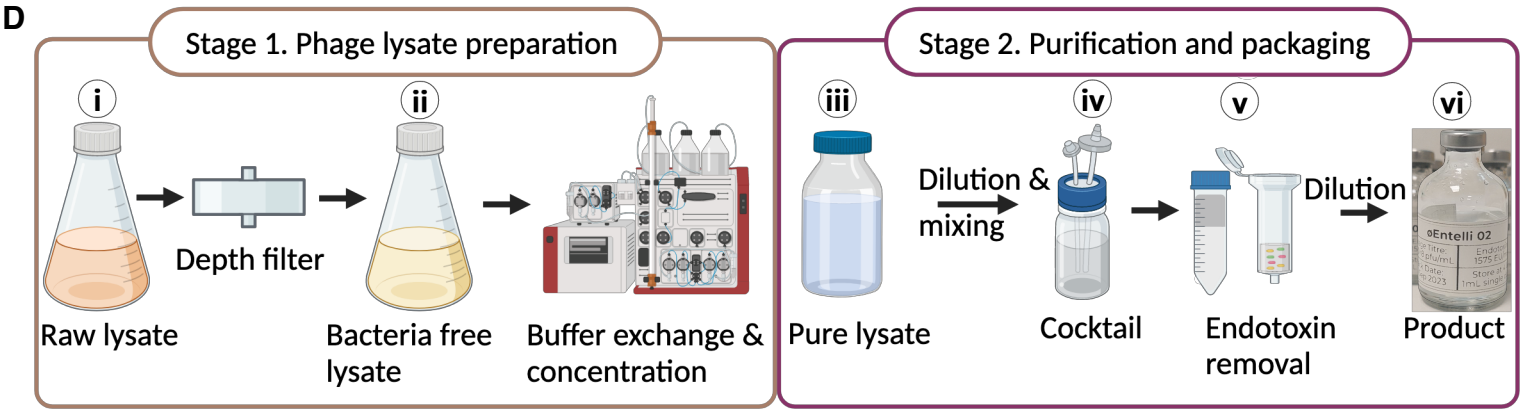
D
Stage 1. Phage lysate preparation
i
ii
Depth filter
Raw lysate
Bacteria free lysate
Buffer exchange & concentration
Stage 2. Purification and packaging
iii
iv
v
vi
Dilution & mixing
Dilution
Pure lysate
Cocktail
Endotoxin removal
Product

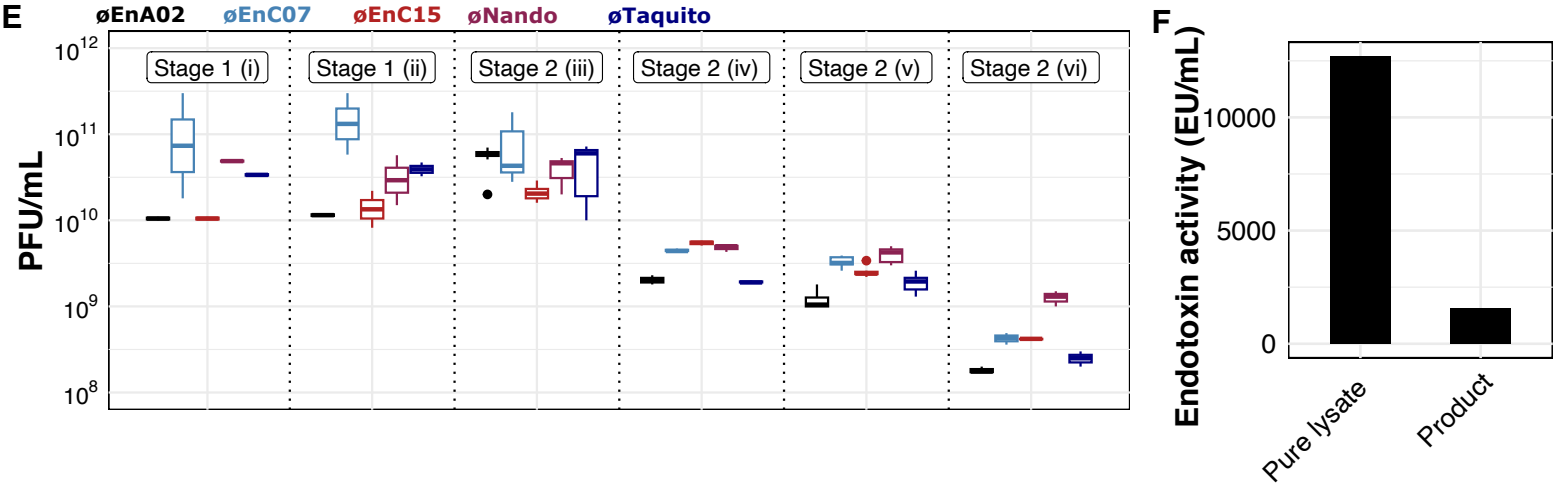
E
øEnA02
øEnC07
øEnC15
øNando
øTaquito
PFU/mL
Stage 1 (i)
Stage 1 (ii)
Stage 2 (iii)
Stage 2 (iv)
Stage 2 (v)
Stage 2 (vi)
F
Endotoxin activity (EU/mL)
10000
5000
0
Pure lysate
Product

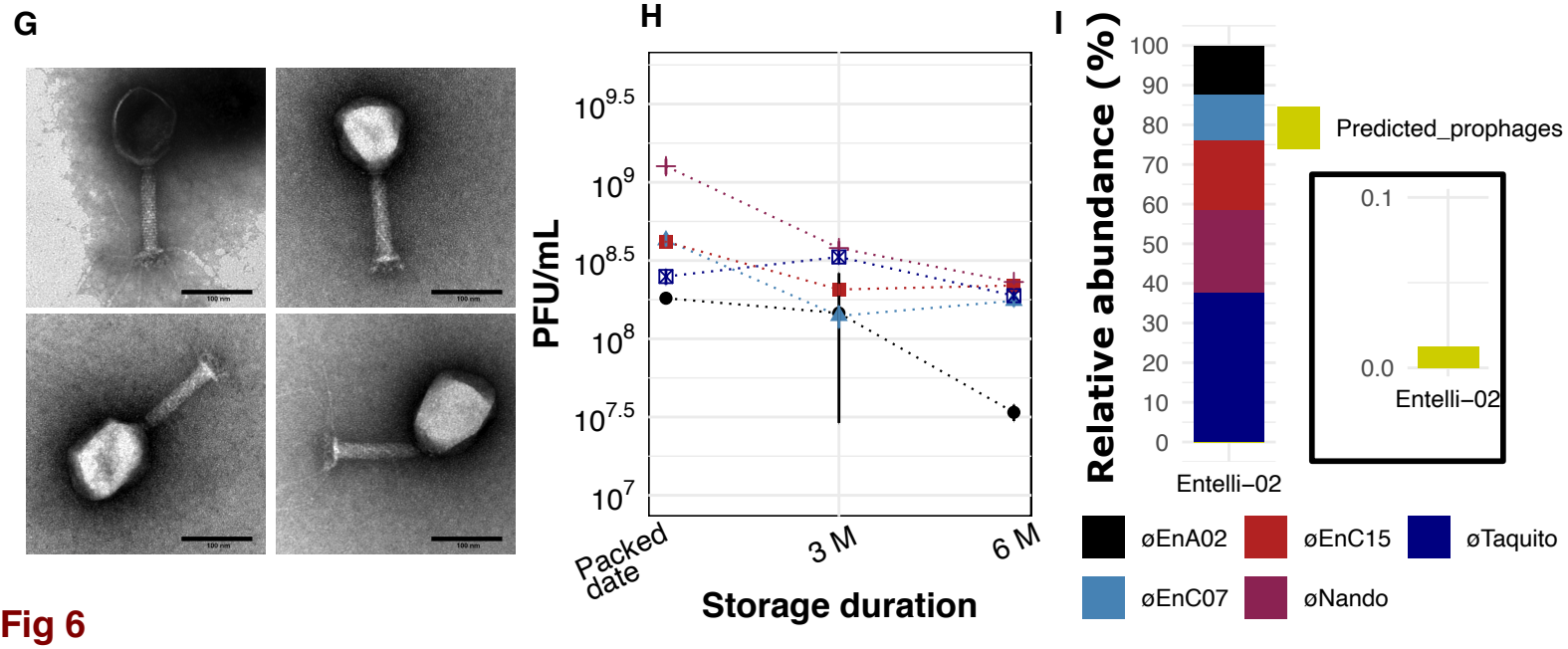
G
H
PFU/mL
Packed date
3 M
6 M
Storage duration
I
Relative abundance (%)
Predicted_prophages
Entelli–02
øEnA02
øEnC15
øTaquito
øEnC07
øNando

Fig 6